UNCLASSIFIED

AD 273 865

Reproduced
by the

ARMED SERVICES TECHNICAL INFORMATION AGENCY
ARLINGTON HALL STATION
ARLINGTON 12, VIRGINIA

UNCLASSIFIED

NOTICE: When government or other drawings, specifications or other data are used for any purpose other than in connection with a definitely related government procurement operation, the U. S. Government thereby incurs no responsibility, nor any obligation whatsoever; and the fact that the Government may have formulated, furnished, or in any way supplied the said drawings, specifications, or other data is not to be regarded by implication or otherwise as in any manner licensing the holder or any other person or corporation, or conveying any rights or permission to manufacture, use or sell any patented invention that may in any way be related thereto.

273865
273 865
CATALOGED BY ASTIA
AS AD NO. _____

[redacted]

This Research is a part of
Project DEFENDER sponsored
by the Advanced Research
Projects Agency

SEMI-ANNUAL REPORT
By: W.H. Wurster & P.V. Marrone
Contract No. ARPA NO. 253-62
CAL Report No. QM-1626-A-2
January 1962

ASTIA
[illegible]
[illegible]
1961

CORNELL AERONAUTICAL LABORATORY, INC.
OF CORNELL UNIVERSITY, BUFFALO 21, N. Y.

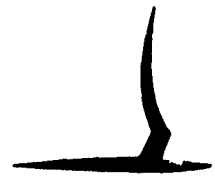

CORNELL AERONAUTICAL LABORATORY, INC.
BUFFALO 21, NEW YORK

REPORT NO. QM-1626-A-2

STUDY OF INFRARED EMISSION FROM HYPERSONIC AIR FLOWS

JANUARY 1962

SEMI-ANNUAL REPORT

BY: Walter H. Wurster

Walter H. Wurster

Paul V. Marrone

Paul V. Marrone

APPROVED BY: A. Kantrowitz

A. Kantrowitz, Head
Aerodynamic Research Dept.

THIS REPORT COVERS WORK PERFORMED UNDER
CONTRACT NO. DA-30-069-ORD-3443,
ARPA ORDER NUMBER 253-62.

FOREWORD

This semi-annual report presents the results and conclusions of the Study of Infrared Emission from Hypersonic Air Flows carried out by the Aerodynamic Research Department of Cornell Aeronautical Laboratory through 31 December 1961. Work on the contract was initiated on 25 September 1961, and hence this report covers a three-month effort. The work was supported under Contract DA-30-069-ORD-3443, ARPA Order No. 253-62. It represents a technical continuation of earlier work on the same research reported in Cornell Aeronautical Laboratory Reports No. QM-1373-A-1, QM-1373-A-2, QM-1373-A-3, and QM-1373-A-4 which cover the period from July 1959 to June 1961.

This report differs from an earlier version (QM-1626-A-1) in that two appendices, representing complete papers, have been replaced by their respective abstracts. The papers are discussed herein, and have been issued as separate Cornell Aeronautical Laboratory reports.

ABSTRACT

This report presents the results obtained through 31 December 1961 of a research program whose objective is to formulate a comprehensive picture of the infrared radiation from re-entry bodies. The program is divided into two phases: the experimental determination of the radiative properties of the optically active gaseous species, and the analysis of the blunt-body flow field, in which the finite-rate chemistry of the air is coupled with the aerodynamics of the flow.

The final analysis of the nitrogen first-positive band spectrum has been completed. The measured intensities are shown to be lower by a factor of five than those reported for measurements in shock-heated air, and the corresponding f-number, evaluated at the $v' = v'' = 0$ band head was found to be $(2.8 \pm .7) \times 10^{-3}$. The nonequilibrium radiation from this $N_2(1+)$ system, arising from the finite rate of electronic excitation has been studied, and a discussion on this topic is presented. In addition, a machine program has been developed which generates the spectra of radiating species from the known spectroscopic constants and the experimentally determined transition probabilities.

The machine program which solves the blunt-body flow-field problem has been modified to streamline the program and to remove minor instabilities, with the result that more accurate body shapes can now be generated by this inverse method. Several re-entry flow calculations were completed, and a nonequilibrium scaling criterion investigated. Several results of these computations are discussed and the scaling criterion is shown to be valid for the IRBM (15, 000 ft/sec) and ICBM (23, 000 ft/sec) conditions which were investigated. Numerical solutions obtained for a parabolic bow-shock shape are compared with those obtained for a catenary shock at the same flight condition. In addition, results obtained from the streamtube program are given and compared with the results obtained with the inverse solution.

TABLE OF CONTENTS

INTRODUCTION

It is the purpose of this research program to extend the knowledge required to formulate a comprehensive picture of the infrared radiation from the shock-heated air about re-entry bodies. The general approach to the problem has been set forth in earlier progress reports[1] generated under the contracts preceding this one. In addition, all experimental details and the formulation of the method of attack have been presented in these reports. Thus, except for a brief discussion for over-all continuity, this report will be restricted to a presentation of the results generated to date on the present contract.

The work has been divided into two primary phases: The division is a natural one, in that the prediction of optical and electrical properties within the gas cap of re-entrant vehicles requires both the coupled chemical and gas-dynamic solutions for the flow field, and the detailed knowledge of how the radiation depends upon the variation of temperature and density given by these solutions. Thus, the radiation measurements phase of the research is directed toward the specific measurements of radiation from the gaseous components of heated air, so that the optical behavior from each of the radiating species is well understood in terms of its basic transition probabilities. In this manner the integrated effect of all the species of the hot air mixture can be determined under the extreme flight conditions unattainable in the laboratory.

Once the transition probabilities are known, there is required the knowledge of the concentration of species within the flow field of a given configuration-trajectory system. This information is derived from the bow-shock machine program that has been developed under this contract. The program is general, in that arbitrary kinetic air models can be used as inputs, and the variation of reaction rates on the solution can be determined. The complete interaction of the finite-rate chemistry of this multicomponent gaseous system with the inviscid gasdynamic flow field is taken into account.

The present status of the research on each phase is covered in detail in subsequent sections of this report. Section I treats the work done under the

radiation measurements phase. The radiation studies on the $N_2(1+)$ system have been completed, and reported in Cornell Aeronautical Laboratory Report No. QM-1626-A-3. The paper has also been accepted for publication in the Journal of Chemical Physics. Because the results are some five times less than those determined from shock-heated air,[2] studies in air and various N_2-O_2 mixtures are presently underway. In addition, the problem of nonequilibrium overshoot radiation of the $N_2(1+)$ system has been examined, and some results obtained. It should be noted that the nonequilibrium radiation resulting from concentrations of radiators which are chemically out of equilibrium as based on the local translational temperature is taken into account in the flow-field analysis. The nonequilibrium due to the finite rate at which the excited electronic states are populated also gives rise to the overshoot radiation. This latter effect was studied, and is discussed in Section IC. Finally, a program is being developed which takes into account the coupling of the results of the two phases. The spectral intensities for the various species are generated from the experimentally determined fundamental constants, and will be combined with the outputs of the flow-field solutions to yield the total radiation from the flow field.

The progress under the blunt-body flow-field analysis phase is presented in Section II. Several refinements of the bow-shock computer solution have been completed. Since the problem involves a two-dimensional integration rather than the one-dimensional integration used for the normal shock, the accuracy of the solution depends on the precision with which derivatives in a direction parallel to the shock are known. Several of these derivative procedures were compared to obtain an optimum routine that is now incorporated in the general bow-shock program. The development of these refinements is discussed. Using the bow-shock solution, several re-entry flow calculations were completed, and a nonequilibrium scaling criterion investigated. An extensive discussion of the results, presented in the light of the over-all nonequilibrium flow-field problem was presented at the National IAS Meeting in New York, January 1962. The abstract of this paper is included as Appendix B.

SECTION I

Radiation Measurements Phase

A primary objective of this phase of the program is the measurement of the absolute infrared spectral intensities from the gases of which shock heated air is composed. The advantage of studying single components rather than the complete mixture has been thoroughly stressed in previous reports.[1] It rests on the fact that the contribution to the over-all spectrum by an individual component varies markedly with temperature and density, in a manner unique to each species. Thus, measurements made on a mixture cannot be reliably extrapolated to conditions other than those under which the measurements were made. On the other hand, basic measurements on the behavior of a given species can yield the fundamental knowledge whereby its radiative behavior can be predicted under arbitrary conditions. Specifically, the transition probabilities or f-numbers for a given band system of a radiating species is a constant unique to that species which gives, essentially, the radiative efficiency for each excited molecule in the mixture. Thus, the transition probability, coupled with the concentration of excited molecules completely specifies the radiant intensity from the gas. An important point to note is that these transition probabilities can be measured under any conditions of convenience , provided that the concentration of emitters is known. Thus, in the shock tube, where gases are processed to thermodynamic equilibrium at high temperatures, the distribution of the molecules in the allowable energy levels is known, and an absolute measurement of the resultant spectrum yields the radiative contribution of each molecule directly. This is the general approach that has been taken on the problem of determining the radiation from shock-heated air.

A. Radiation Experiments

In the near infrared, one of the significant radiating systems is the first-positive band system of nitrogen. It was the first object of experimental study, and in the last annual report[1] of the previous contract the measured spectrum from this band system was reported. During the past quarter, these data were analyzed in detail, and the results are now in the process of publication. The abstract of the paper has been included in this report as Appendix A. The paper has also been presented as a separate Cornell Aeronautical Laboratory report[6] for broader distribution, as the results are significant in the problem of the contribution of the radiation from nitrogen to the spectrum of heated air.

The conclusions of the nitrogen study may be summarized as follows: The measurements of the spectral intensity of the radiation from pure shock-heated nitrogen are about five times less than those reported by Keck, et al.[2] Their measurements were made on shock-heated air, and the radiation in the near infrared was attributed to the nitrogen first-positive system. The measurements were not made with a spectral resolution capable of identifying the spectral characteristics of the nitrogen. In the present study with pure nitrogen, the spectra were easily identified, and, in fact, the wavelength resolution was sufficient to detect the presence of another radiating system, which was shown to be accounted for by either the CN red band system or the nitrogen ion N_2^+ Meinel band system. In spite of this secondary radiating component, the transition probability for the $N_2(1+)$ system was determined, by virtue of the separation of spectra afforded by the wavelength resolution. The N_2^+ Meinel system has previously been suggested[3] as a possible radiator in high-temperature air, but the present results show that this is definitely not the case. Details of the data reduction and the numerical results may be found in Ref. 6.

It was then decided that a set of experiments be performed in order to determine the origin of the secondary radiating component of the pure N_2 spectrum. This was done by examining the spectrum between 0.8 and 1.1 microns in detail (see Fig. 1) for a set of experiments in which the temperature

and density of the nitrogen was varied over broad limits. In this manner, the measured radiation intensities could be correlated with the corresponding concentrations of N_2 and N_2^+ in the gas, because the radiation must scale directly with the number density of the responsible emitters. It was found that while the intensity of the spectrum at positions corresponding to band heads of N_2, such as 0.88 and 1.04 microns, behaved properly with the N_2 concentrations, the radiation in the band heads of the secondary component, at 0.93 and 1.11 microns, bore no relationship to the N_2^+ concentration. In addition, the time dependence of the radiation at these two latter wavelengths was different in character from that of the N_2 records. For these reasons it was concluded that the secondary component of the radiation must be interpreted as originating from a CN impurity. Assuming a reasonable transition probability for the CN system, the radiation can be accounted for by a concentration of one part in 10^5. Although this level of impurity is higher than that of the original test gas, it could reasonably be attributed to impurities driven from the shock tube walls at these extreme temperatures. These results demonstrate the importance of using as high a spectral resolution as possible for measurements of this type so that the effect of such small but highly efficient impurity radiators may be distinguished.

Measurements in pure nitrogen have been concluded, and the present experimental program is directed toward spectral measurements in air and various N_2-O_2 mixtures. By scaling the measured intensities with the possible radiating species, the origin of the radiators can be uniquely identified. This particular set of experiments has not been completed, but will be presented shortly in a separate report.

B. Computation of the Radiation from the Shock-Heated Flow Field

As has been discussed earlier, the outputs of the results from the two phases of the research program will be coupled to yield the emission spectrum from the gas cap of re-entrant vehicles.

The output of the flow-field program will essentially comprise a map, which gives, for each volume element in the gas cap, the thermodynamic properties of pressure, density, and temperature, the concentrations of all species: molecular, atomic, and ionic. In addition, the local vibrational temperature for the diatoms is calculated. It is planned to modify the program slightly, so that the distribution of the radiating species in the pertinent electronic energy levels is contained in the printed output. At the present time, the electronic excitation rates will be assumed infinitely fast, so that the distribution in electronic energy levels will be determined only by the local translational temperature. When sufficient data become available on these excitation mechanisms and rates, they can be readily incorporated as another reaction in the program. The present state of knowledge of such rates does not warrant their inclusion at this time. Vibrational excitation rates for the ground electronic state are already contained in the bow-shock program.

In general, the spectrum of a given band system from a single radiating species extends over a broad wavelength range, and the radiated intensity from air at a given wavelength requires the summation over the individual contributors. To facilitate this calculation, a separate computer routine was developed, in which the spectrum from a given species could be generated from fundamental spectroscopic constants. The position of the band heads are well known. In the program these are generated from the known molecular constants, and the distribution of intensities of the various bands are obtained from published values of the overlap integrals for the molecule. A simplified band shape was assumed to be sufficient for these calculations, and the bands were taken to be Q-form and smoothly contoured. This band model was also taken in the analysis of the nitrogen results. It is discussed in Ref. 6. In Fig. 1 the spectrum predicted by such a model can be seen. The band heads are more sharply peaked than would actually occur, but in the regions of multiple heads and at

higher temperatures the resultant contours will approach the actual spectrum more closely. It is interesting to note that the computer-generated spectrum, automatically taking into account more bands than were used in the hand calculation of the $N_2(1+)$ spectrum of Fig. 1 revealed a correction to the spectrum at 0.90 and 1.06 microns which matched the experimental data points.

With this routine now completed, it is a simple task to generate a complete spectrum correctly scaled in intensity, given the temperature and the number density of molecules in the emitting electronic level. The temperature determines both the shape of the band tails and the distribution of molecules in the vibrational energy levels. The two factors which scale the entire spectrum in intensity are then the electronic population, calculated in the bow-shock program, and the pertinent transition probabilities, which are the objectives of the experimental radiation measurements portion of the contract. It should be mentioned that an entire spectrum can be calculated by machine in one minute.

Thus, the spectral intensity from the air contained in a volume element of the gas cap around a re-entry vehicle can be directly determined by summing the individual spectra from each species as discussed above. The method for the final summation over all band systems for the total gas cap volume of a given flight configuration presents only a relatively simple machine-routine problem, and shortly will be incorporated in the program.

C. Nonequilibrium Radiation

For all conditions of ICBM re-entry, there are a group of chemical reactions which are not important for the determination of the temperature and density of the air, but which directly determine the magnitude of the nonequilibrium radiation. These reactions are those which have to do with the rate of population of excited electronic states, whose spontaneous decay supplies the optical radiation. Relatively little is at present known about the rate constant for these reactions, or, in fact, even about the mechanism for excitation. After the transition probabilities are known for any optical transition, and the temperature-density history is known behind the bow-shock, the mechanism and rate of excitation are required in order to calculate the nonequilibrium radiation. In the present discussion it will be shown that if one chooses a mechanism of excitation by a one-step process from chemical species whose history is known, and there is a considerable overshoot radiation, then the total nonequilibrium radiation from this particular band system can be calculated without a knowledge of the reaction rate constants. It is also shown that this provides a "radiation plateau", where the total radiation is independent of the pressure in front of the shock wave.[4] The results are illustrated in terms of the nonequilibrium radiation from the $N_2(1+)$ system in the red and infrared region of the spectrum.

The assumption that excited electronic states of nitrogen ($B^3\Pi$ for $N_2(1+)$ radiation) are formed behind the shock wave by collision of N_2 molecules with other species (M) leads to the following chemical equation for the rate of increase of concentration of $N_2^* \equiv N_2(B^3\Pi)$:

$$\frac{d[N_2^*]}{dt} = k_f[N_2][M] - k_r[N_2^*][M] - A[N_2^*] \qquad (1)$$

where k_f and k_r are the (unknown) forward and reverse rate constants for the reaction, A is the known Einstein coefficient for spontaneous emission of the $N_2(1+)$ radiation, and $[N_2]$ and $[N_2^*]$ are the number of N_2 molecules

in the ground and excited states. In terms of the distance behind the shock y a substitution can be made: $dt = (1/v)\,dy$, where V is the velocity of the gas relative to the shock. The equation can then be rewritten

$$[N_2^*] = \left(\frac{k_f}{k_n + \frac{A}{[M]}}\right)[N_2] - \left(\frac{V}{k_n[M] + A}\right)\frac{d}{dy}[N_2^*]$$

The first term on the right is the "local equilibrium" value of $[N_2^*]$- i.e., the value that $[N_2^*]$ would have if the gas were kept at the local temperature $T(y)$ for an indefinite time. Then this can be written

$$[N_2^*]_{LE} = [N_2]\left(\frac{k_f/k_n}{1 + \frac{A}{[M]k_n}}\right) = [N_2]\,\frac{g_u/g_l\, e^{-\frac{h\nu}{kT}}}{1 + \frac{A}{[M]k_n}}$$

where $g_u/g_l\, e^{-h\nu/kT}$ is the equilibrium constant for the upper and lower level, and can be calculated directly. In the altitude range where $\frac{A}{[M]k_n} \ll 1$, the radiation does not seriously drain the excited state, and the quantity $[N_2^*]_{LE}$ can be calculated without knowledge of the rate constants. At higher altitudes (smaller values of M), the radiation is "collision limited" and the correction term in the denominator must be taken into account.

The total radiation per cm^2 from the shock front due to this band system is equal to

$$I = 1.62\times10^{-14}\int_0^Y [N_2^*]\,dy = 1.62\times10^{-14}\left\{\int_0^Y [N_2^*]_{LE}\,dy - \int_0^Y \frac{V}{k_n[M]+A}\,d[N_2^*]\right\} \qquad (2)$$

where I is expressed in watts/cm^2 and $[N_2^*]$ in molecules/cm^3. Y is the depth of the shock layer being considered. The second integral on the right has the value

$$\int_0^Y \frac{V}{k_n[M]+A}\,d[N_2^*] = \bar{L}\,[N_2^*(Y)]$$

where $\bar{L}$ is a mean value of $\frac{V}{k_1[M]+A}$

and is a relaxation distance whose magnitude is of the order of nonequilibrium zone. $[N_2^*(Y)]$ is the concentration of excited nitrogen molecules at the position Y. If the region of integration considered includes the full relaxation distance, this term is equal to the radiation that would obtain if there were no nonequilibrium processes involved. In any case, where there is considerable nonequilibrium overshoot, it is clear that this term is negligible compared with the other two terms in Eq. (2), and so can be ignored. The total nonequilibrium radiation is then equal to that calculated by considering the $[N_2^*]$ to remain in local equilibrium behind the shock wave. Thus, to good approximation

$$I = 1.62 \times 10^{-14} \int_0^Y [N_2^*]_{LE} \, dy \qquad (3)$$

A further simplification in the calculation can be obtained from the fact that for a given velocity, $[N_2^*]_{LE}$ scales directly with the pressure in front of the shock. This is illustrated in Fig. 1, where the quantity $[N_2^*]_{LE}/[N_2^*]_{LE_0}$ is plotted vs. $[N_2^*]_{LE_0} \times Y$ for three cases of different initial pressures and the same flight velocity (23,000 ft/sec.). These results are taken from the normal-shock nonequilibrium IBM program. $[N_2^*]_{LE_0}$ is the value of $[N_2^*]_{LE}$ immediately behind the shock. Since at this point the gas is still treated as an ideal gas, the value of $[N_2^*]_{LE_0}$ is directly proportional to the density ahead of the shock for any given shock speed. It follows that the integral in Eq. (3) is independent of initial pressure, i.e., independent of altitude. This feature has been referred to as the "radiation plateau" for nonequilibrium radiation.[4] The value of the integral is given in Fig. 2 as a function of flight velocity for the $N_2(1+)$ system, both as calculated for pure nitrogen shocks and for shocks in air. The lower value of the radiation from air is related to the more rapid drop in temperature because of oxygen dissociation.

In all cases, the curves shown in Fig. 2 must be considered as upper limits to the nonequilibrium radiation involved with re-entry, because both the effects of competitive reactions (in place of Eq. (1)) and the effects of collision limiting, tend to decrease these values. Clearly, however, the results suggest a direct method of correlating the total measured non-equilibrium radiation with the mechanism which causes the electronic excitation.

SECTION II

Re-Entry Body Flow Field Analysis Phase

The solution of the inviscid nonequilibrium blunt-body problem (which has been discussed previously in Ref. 1) is needed to predict the history of radiation from the hot gas surrounding a re-entry vehicle. The present solution is based on the inverse method (i.e. shock shape and size is prescribed) and employs coupled vibration-dissociation reactions to describe the state of the gas behind the bow-shock wave. This general bow-shock problem has been programmed for an IBM-704 computer. In addition, a similar finite-rate solution has been programmed for normal shock waves to assess the variation of rate constants on the over-all relaxation zone. A description of typical results obtained to date, and numerical refinements of the bow-shock program will be discussed.

The Bow-Shock Solution

The inverse method of solution is used to determine the nonequilibrium flow field around the nose of a hypersonic vehicle. Consider the sketch:

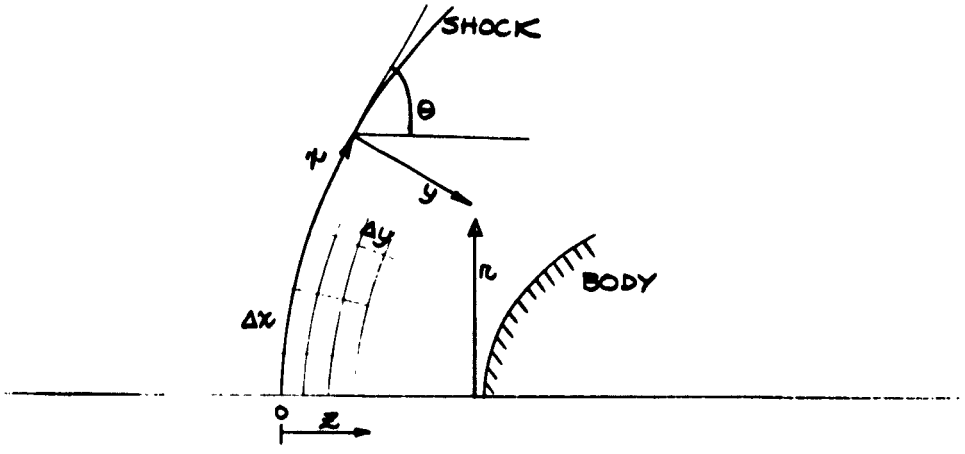

where x is the distance along the shock and y is the coordinate normal to it. The shock is divided into n values of Δx as shown, and the conditions immediately behind the shock are determined from local normal shock

considerations. Once these starting values have been obtained, the entire solution advances forward one Δy interval normal to the shock. The solution cannot proceed forward one ray χ_m at a time, since the derivatives in the χ direction parallel to the shock are needed. These represent the flow swept by a point on any given ray, since the rays do not follow streamlines, but cross them. The accuracy of the solution depends to a great degree on the precision with which these χ derivatives are known. At the initiation of the present contract, the re-entry body flow-field analysis phase had developed to the point where complete solutions up to about 70° from the centerline had been obtained. However, the machine program was limited in obtaining accurate body shapes and flow-field solutions close to the body because of numerical difficulties in this regime. Thus, emphasis has been placed on refining the bow-shock program to obtain more accurate solutions and body shapes. This involved programming a more sophisticated χ-derivative fit than had previously been used.

The early results shown in Ref. 1 were obtained using a simple parabolic fit to the variables along 3 points in the χ direction, with the derivative being taken at the center point (i.e. 3-point fit). A simple linear fit was used on the end rays. As indicated in Ref. 1, a slight waviness in the body shape, as computed from mass conservation relations, was observed. These inaccuracies were most noticeable on the end rays. A more precise description of the variables over a larger arc in the χ direction would, in effect, be a smoothing procedure and lead to more accurate body shapes. Thus, a number of χ-derivative subroutines were developed to assess the optimum fit to be used in the final bow-shock program. These included: a refined 3-point parabolic fit on all rays, including the end rays (3-point fit); a polynomial fit covering 5 points in the χ direction (5-point fit); and a least squares quartic fit through 7-points (7-point fit). A series of bow-shock computations for an ideal gas ($\gamma = 1.4$) and a dissociating simple diatomic gas (oxygen) were performed with the various χ-derivative fits, to assess their effects on the flow-field solutions and final body shapes.

The most noticeable inaccuracy in the resultant body shapes discussed in Ref. 1 was the small spike appearing near the stagnation point (i.e., end rays near the centerline). With the use of higher order x-derivative fits, this spike disappeared. This can be seen in Fig. 4, which shows the nose region of a body computed for the ideal gas case. A shock Mach number of 14 was specified for the given catenary shock of 0.5 centimeter nose radius. The early 3-point routine with linear fit on the end rays shows the most pronounced spike. A gradual decrease of this spike, along with a general smoothing of the body surface is seen as the higher order fits are used. Thus, to minimize inaccuracies in the flow field and body shape in the stagnation region, the 7-point fit is the most desirable. This same smoothing effect occurred for the oxygen calculations, as well as for several non-equilibrium air computations using the different fits.

Numerical problems of a different nature predominate on the outermost rays. Here, inaccuracies in the solution are manifested as oscillations along the outermost rays which propagated down into the flow field by way of the x derivatives. In general, a large number of Δy steps were needed to proceed from the shock to the body for the air solutions, enabling these oscillations to propagate well into the flow field. Lick[5] dealt with this problem by starting with a large number of rays (i.e. Δx values) and dropping the outermost points after each successful integration interval. Thus, his computed flow-field solution resembled the following sketch:

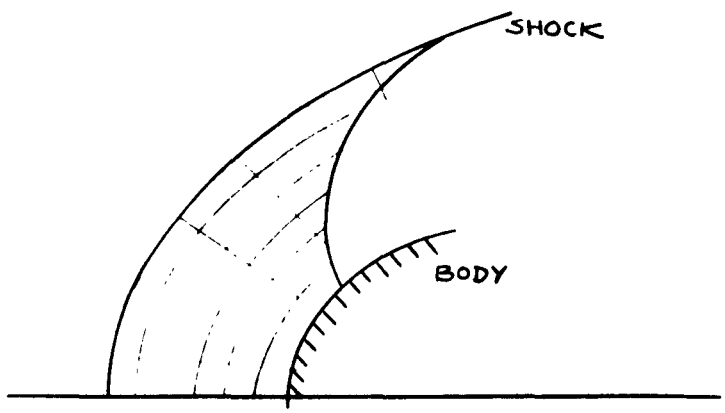

This method becomes prohibitive in terms of machine computation time when dealing with air, due to the large number of Δy intervals needed (i.e., perhaps 30 steps as compared to 10 steps or so for Lick's diatomic gas solution). A large number of Δy intervals in turn requires a large number of rays initially so as to end up with a reasonable portion of the flow-field solution. Nonetheless, this procedure of dropping end points is the most accurate method of solution, and will eliminate unwanted numerical instabilities from propagating into the flow field. Thus, the refinement of dropping the two outer end points with each successful integration step was incorporated into the 5-point and 7-point fits to act as standards with which to compare less time consuming methods. In general, it was found that the more sophisticated higher order fits with no dropping of end points led to greater discrepancies from these standards than did the refined 3-point fit. In addition, the 3-point fit gave the most stable solution (aside from the end point dropping routines). This is shown in Figs. 5 and 6. Figure 5 shows the density distribution around the body (i.e., increasing values of x) for the ideal gas case. The 5-point fit with dropping of end points is the standard for comparison here. It may be noted that the 7-point end dropping routine gave an almost identical solution. The density distribution is shown for three values of y/R_s (increasing from shock to body). For $y/R_s = 0.108$, the results of solutions with other x derivative routines are given as a comparison. The higher order fits with no end point dropping, (i.e. $x/R_s = .78$ is the last ray), show a falling off from the standard distribution. As the solution proceeds to larger values of y/R_s, this discrepancy propagates back into the flow field (decreasing values of x/R_s) at a fast rate. The refined 3-point fit solution, however, is seen to fall extremely close to the standard. Figure 6 points out this same phenomenon for the reacting diatomic gas case. Here, the 7-point end point dropping solution is to be used as the standard. Again the simple 3-point fit results agree extremely well with the standard solution ($x/R_s = .78$ is again the last ray for the 3-point solution). The final x-derivative routine decided upon to be used in the general bow-shock program consists of the 7-point fit over the major part of the flow field (to insure accurate solutions and body

shapes near the stagnation region), with the 3-point fit on the outer rays (to insure accuracy at the outermost part of the flow field). This fit gives the most stable and accurate solutions consistent with reasonable machine computation time. Differences of less than 0.1% in the variables along the outer rays, when compared with the higher order end point dropping procedures, were the maximum deviations encountered.

An additional complication in the early bow-shock solutions arose when the first ray (i.e. ray nearest to the centerline) reached the body. Numerical difficulties leading to program test failures occurred when the solution was carried into the body. A new routine has been completed that carries the solution along each ray until the body is reached. From that point on, that particular ray is uncoupled from the flow-field calculation, and the 7-point χ-derivative fit slides up to the next ray. With this procedure, flow solutions close to the body, as well as accurate body shapes are computed.

Bow-Shock Results

The 7-point plus 3-point χ-derivative fit on the outer rays was incorporated into the general bow-shock program, as was the ray uncoupling procedure. This refined bow-shock solution was then used in a series of IRBM (velocity of 15,000 ft/sec) and ICBM (velocity of 23,000 ft/sec) flow-field calculations to study the nonequilibrium phenomena in the shock layer, and to test the validity of a scaling criterion for nonequilibrium flows.

The results of these computations are extensively discussed in Ref. 7, which was presented at the National IAS Meeting in New York, in January 1962. It is felt that the significance of the bow-shock and streamtube results can best be appreciated when presented in the light of the over-all flow-field problem, thus indicating the present state of knowledge concerning nonequilibrium airflows. The abstract of this IAS paper is included as Appendix B. However, a discussion of some of the numerical results is included in this report as an indication of the type of solution that is obtained with the bow-shock program.

The solutions for both cases (IRBM and ICBM), as presented, not only give an insight into the characteristics of the nonequilibrium shock layer, but also serve to establish the validity of a nonequilibrium scaling law proposed

by Gibson.[8] Since it is extremely difficult to obtain nonequilibrium flow-field measurements in free-flight vehicles, ballistic ranges and hypersonic tunnels have been developed as tools to aid in the determination of hypersonic flow fields. However, the models used in these devices are generally much smaller than full scale which precludes the duplication of the finite-rate chemistry about the body. Thus, a valid nonequilibrium scaling law must be used to relate ballistic range and hypersonic tunnel data with corresponding free-flight conditions if meaningful data are to be obtained from these facilities. One of the most useful purposes of an exact numerical solution for the finite-rate flow field is that it serves as a standard, with which simpler and more approximate methods may be compared.

Such a nonequilibrium scaling criterion is extensively discussed in both Refs. 7 and 8, and will only be briefly described here. For flight conditions where the three-body recombination reactions are unimportant, as in most high-altitude nonequilibrium shock layer flows, the chemical relaxation phenomena is governed by two-body processes and binary scaling is possible. Thus, for a given flight velocity, the inviscid nonequilibrium shock layer around a blunt-nosed vehicle will be scaled if the condition $\rho_\infty R$ = constant. Here ρ_∞ is the ambient atmospheric density, and R is a characteristic dimension of the vehicle (i.e. R_b is body radius). For the bow-shock program, this is equivalent to $\rho_\infty R_s$ = constant, where R_s is the bow-shock radius of curvature at the centerline.

All flow-field solutions were computed using an 8 species (O, N, e^-, Ar, O_2, N_2, NO, NO^+), 10 reactions air model as follows:

1. $O_2 + O \underset{k_{R_1}}{\overset{k_{F_1}}{\rightleftharpoons}} 2O + O$ $\qquad k_{F_1} = 2.1 \times 10^{18} T^{-.5} \exp\left[-\frac{59380}{T}\right] \frac{cm^3}{mole\text{-}sec}$

2. $O_2 + O_2 \underset{k_{R_2}}{\overset{k_{F_2}}{\rightleftharpoons}} 2O + O_2$ $\qquad k_{F_2} = 3.6 \times 10^{21} T^{-1.5} \exp\left[-\frac{59380}{T}\right]$

3. $O_2 + M \underset{k_{R_3}}{\overset{k_{F_3}}{\rightleftharpoons}} 2O + M$ $\qquad k_{F_3} = 1.19 \times 10^{21} T^{-1.5} \exp\left[-\frac{59380}{T}\right]$

4. $N_2 + N \rightleftharpoons 2N + N$ $\quad k_{R_4} = 7.5 \times 10^{20} T^{-1.5}$

5. $N_2 + N_2 \rightleftharpoons 2N + N_2$ $\quad k_{R_5} = 1.5 \times 10^{20} T^{-1.5}$

6. $N_2 + M \rightleftharpoons 2N + M$ $\quad k_{R_6} = 5 \times 10^{19} T^{-1.5}$

7. $NO + M \rightleftharpoons N + O + M$ $\quad k_{F_7} = 5.18 \times 10^{21} T^{-1.5} \exp\left[-\frac{75490}{T}\right]$

8. $N + O_2 \rightleftharpoons NO + O$ $\quad k_{F_8} = 1 \times 10^{12} T^{0.5} \exp\left[-\frac{3120}{T}\right]$

9. $O + N_2 \rightleftharpoons NO + N$ $\quad k_{F_9} = 5 \times 10^{13} \exp\left[-\frac{38016}{T}\right]$

10. $N + O \rightleftharpoons NO^+ + e^-$ $\quad k_{R_{10}} = 1.8 \times 10^{21} T^{-1.5}$

In addition, vibrational equilibrium was assumed for these computations, which were carried approximately 60° off the centerline for a catenary shock. The effect of vibrational nonequilibrium, and the coupling of vibration and dissociation has been investigated behind strong normal shock waves in air.[7] Upon refinement of the vibrational nonequilibrium subroutine for the inverse solutions, these studies will be extended to the bow-shock flow field. These solutions will indicate the degree of interaction between these processes around the nose cap of a high-altitude vehicle. The present assumption of vibrational equilibrium does not affect the scaling of the nonequilibrium chemistry, since vibrational nonequilibrium will also scale directly as density.[7]

For the IRBM (15, 000 ft/sec) flight condition, the flow field around the nose of a one-foot radius vehicle at an altitude of 200, 000 feet was computed. This calculation was repeated for a scaled vehicle at a higher and lower altitude, 250, 000 and 150, 000 feet respectively, with the product $\rho_\infty R_s$ held constant. The cases computed are seen in the table, where the 1956 ARDC atmosphere was employed:

Flight Velocity	Altitude	Shock Radius	Standoff Distance
15, 000 fps	150, 000 ft	0. 183 ft	0. 0686
15, 000	200, 000	1. 07	0. 0676
15, 000	250, 000	8. 15	0. 0681

As can be seen from the table, the shock standoff distance for the three computations agree to about 1%. Figure 7 shows the body shapes obtained in the normalized axisymmetric coordinate system. The correlation is excellent, with the resultant body shapes spherical to within a few per cent at an angle of approximately 60° off the centerline. Results for the temperature, nitric-oxide and electron distributions are shown in Figs. 8 - 10 for two rays normal to the shock (approximately 9° and 35° off the centerline). The results from all three computations are shown on each figure and are plotted as a function of distance (y) normal to the shock divided by the local standoff distance (δ). It is seen that the flow fields are in fact identically scaled. The temperature is seen to decrease towards equilibrium stagnation from about 8500°K immediately behind the strong portion of the shock near the centerline. An overshoot in NO concentration, typical of shock relaxation phenomena in air, is observed, and the gradient in electron concentration from the shock to the body is clearly seen.

Similar flow-field computations for ICBM (23, 000 ft/sec) flight conditions were performed. The flow field around a one-foot diameter vehicle at 250, 000 feet altitude was scaled at 200, 000 feet, as shown in the table:

Flight Velocity	Altitude	Shock Radius	Standoff Distance
*23, 000 fps	250, 000 ft	0. 525 ft	0. 0666
23, 000	200, 000	0. 0692	0. 0670

* Results for this case are from computations performed for the Air Research and Development Command, Rome Air Development Center, Griffiss Air Force Base, New York, under Contract No. AF 30(602)-2267.

Again the standoff distances agree very well, and Fig. 11 shows the excellent correlation of the two body shapes. The temperature, NO and electron concentrations given in Figs. 12 - 14 show that the two flow fields are identically scaled. The temperature gradient is quite extreme for this higher velocity case, decreasing from approximately 18, 000°K behind the shock near the centerline to approximately 6000°K in the stagnation region. In addition, the extreme overshoot in electron concentration is easily observed.

Variation of Bow-Shock Shape

All flow-field solutions to date have had prescribed a catenary shape for the bow-shock wave. The resultant body shapes have been spherical to within a few per cent at angles to approximately 60° off the centerline. However, it is of practical importance to investigate the flow fields produced by various re-entrant body shapes. Since the inverse method is utilized in the bow-shock solution, this is equivalent to varying the shock-wave shape. Shock shapes which close less rapidly than a catenary (i. e. parabola), may produce body shapes which more closely approximate actual sphere-cone configurations which are still spherical in the subsonic nose cap region, but become conical at higher angles. Thus, preliminary computations have also proceeded for shock shapes other than the catenary. A parabolic shock shape has been programmed, and to date, one calculation with this shock has been completed and compared with results obtained from a catenary shock solution. This was done for the one-foot diameter body traveling at 15, 000 feet per second at an altitude of 200, 000 feet. The same rate data were employed. Figure 15 shows the two shock shapes in the normalized axisymmetric coordinate system. The parabola is seen to lie quite close to the catenary for angles less than about 45° off the centerline, thereafter lying above it. The present calculation was carried to approximately 60° off the centerline. Figure 16 shows the resultant body shapes in the normalized shock coordinate system. For values of $\frac{x}{R_s} < 0.6$ ($\theta \approx 35°$), the body shapes are nearly identical. The standoff distances, for example, are within 1% ($\frac{\delta}{R_s} = .0676$ for catenary, $\frac{\delta}{R_s} = .0683$ for parabola). At higher angles, the body generated by the parabolic shock lies above that obtained for a catenary shock (i. e. the y_{body} values are nearly identical, and the parabolic shock lies above the catenary). The flow fields were

compared along the two rays previously discussed (i. e. 9° and 35° off the centerline) and found to be essentially identical. Comparison of the flow fields and body shapes for higher angles are presently underway. But it can be said in general that in the subsonic position of the flow field, the parabolic and catenary shocks give almost identical solutions.

Streamtube Solution

The bow-shock solution describes the flow field around the nose cap of a re-entering body, and as such is a necessary starting point for determination of the flow field around the afterbody of a hypersonic vehicle. One method of coupling this solution with the afterbody flow is with the streamtube method of solution, i. e. each streamline emerging from the sonic line in the shock layer may be considered as a quasi-one-dimensional streamtube for an expanding flow. A numerical solution for the surface streamline has been developed to give an indication of the flow properties near the surface of the afterbody. This streamtub solution is a modification of a nonequilibrium quasi-one-dimensional program developed at Cornell Aeronautical Laboratory for nozzle expansions.[9] Again, this is extensively discussed in Refs. 7 and 10 and will only be briefly described here. A prescribed pressure distribution on the surface of the vehicle is used to obtain the surface streamtube area distribution used in the solution. It is the streamtube which starts at stagnation-point equilibrium conditions. A modified Newtonian pressure distribution was assumed from the stagnation point to the body shoulder, where the ratio of shoulder to stagnation pressure was taken to be about 0. 05. The first-order form of the blast-wave theory was employed for the afterbody pressure distribution, with the body shoulder chosen as the match point.

Streamtube Results and Comparison with Bow-Shock Results

Results for a hemisphere-cylinder configuration (15, 000 ft/sec; 200, 000 feet altitude, body radius equal to one foot) are shown in Figs. 17 and 18 where the nonequilibrium temperature, NO and electron concentrations are compared with the corresponding equilibrium solution. These results are for the surface streamtube starting at the equilibrium stagnation conditions of 4767°K and 0. 062 atm pressure. The temperature obtained from the nonequilibrium solution is seen to be considerably below that obtained from the equilibrium solu-

tion due to the energy remaining frozen in the flow in the finite-rate solution. The electron concentration along the afterbody, however, is almost two orders of magnitude above that predicted from equilibrium considerations, due to the freezing of the electrons near the shoulder. A considerable undershoot below the equilibrium value is seen in the NO concentration along the afterbody, again amounting to over two orders of magnitude. A comparison of the results obtained with the streamtube solution with those obtained from the bow-shock program was presented in Ref. 11. Figure 19 shows the comparison for the electron concentration along the body surface; the agreement is very good, to within 5%. This same sort of agreement is also obtained for the atomic species O and N.

However, the agreement is substantially different for O_2, N_2, NO and T close to the stagnation region. This is due, in general, to the extreme gradients in these quantities extremely close to the body surface in this region. To accurately compute these concentrations with the bow-shock solution would be very time consuming. The fact that these large gradients only exist very close to the surface (about the last 1% or less of the y distance in the bow-shock program) enables an accurate prediction of some 99% of the nonequilibrium shock layer with the bow-shock program. To avoid these gradients in practice, the ray uncoupling procedure previously described, is employed when any given ray reaches 99% of the distance to the body. In order to determine the effect of this cut-off procedure, a small section of the flow field (up to about 15° off the centerline) near the stagnation region was computed in great detail with the bow-shock solution. Very small step sizes for integration in the y direction (1/100 to 1/1000 of the standoff distance) were required for the last 1/2% of the distance from the shock to the body. Close agreement with the streamtube results in the stagnation region was then obtained. However, the length of computing time required is not considered to be worthwhile to obtain an accurate solution of this small region with the inverse method, since the streamtube program can be utilized if needed, to provide a solution close to the body in the stagnation region.

Summary

The bow-shock program is essentially complete, and a great number of flow-field solutions have been obtained, both for flight and hypersonic tunnel conditions. Flow-field computations for both IRBM (15, 000 ft/sec) and ICBM (23, 000 ft/sec) conditions have shown the validity of a nonequilibrium scaling criterion, which can be used to relate ballistic range and hypersonic tunnel data with free-flight conditions. Preliminary computations for shock shapes other than the catenary show a close agreement in the subsonic flow-field solutions for a parabolic and a catenary shock. The surface streamtube solution, starting at the stagnation point, is completed and has proven to be a valuable tool in predicting the flow field near the afterbody surface, and also serves as a comparison for the bow-shock solutions at the body surface.

At the present time, the vibrational nonequilibrium subroutine for the bow shock is being refined. When this is completed, flow-field computations will be performed to assess the effect of the coupled vibration-dissociation air model on the complete blunt-nose flow field at high altitudes. The limitations of the range of application of the bow-shock program imposed by viscous terms at high altitudes are being examined. The extension of solutions to include the viscous problem is being considered under this and other contracts at this Laboratory. In addition, the range of validity of the scaling criterion is being investigated, especially in the neighborhood of the stagnation region, where the inviscid flow approaches equilibrium.

REFERENCES

1. Wurster, W. H. and Marrone, P. V., Study of Infrared Emission in Heated Air. Cornell Aero. Lab. Repts. QM-1373-A-1, QM-1373-A-2, QM-1373-A-3, and QM-1373-A-4, through June 1961.
2. Keck, J. C., Camm, J. C., Kivel, B., and Wentink, T., Jr., Ann. Phys., 7, 1, 1959.
3. Meyerott, R. E., Sokoloff, J., and Nicholls, R. W., Absorption Coefficients of Air. Geophys. Res. Papers No. 68, GRD-TR-60-277, July 1960.
4. Teare, J. D., Georgiev, S., and Allen, R. A., Radiation from the Nonequilibrium Shock Front. AVCO Res. Rept. 112, October 1961.
5. Lick, W., J. Fluid Mech., 7, Pt. 1, 128, January 1960.
6. Wurster, W. H., Measured Transition Probability for the First-Positive Band System of Nitrogen. Cornell Aero. Lab. Rept. QM-1626-A-3, January 1962.
7. Hall, J. Gordon, Eschenroeder, A. Q., and Marrone, P. V., Inviscid Hypersonic Air Flows with Coupled Nonequilibrium Process. IAS Paper No. 62-67, presented at IAS Annual Meeting, New York, January 1962.
8. Gibson, W. E., Dissociation Scaling for Nonequilibrium Blunt-Nose Flows. ARS Journal, Vol. 32, No. 2, pp. 285-287, February 1962.
9. Eschenroeder, A. Q., Boyer, D. W., and Hall, J. G., Exact Solutions for Nonequilibrium Expansions of Air with Coupled Chemical Reactions. Cornell Aero. Lab. Rept. AF-1413-A-1, May 1961.
10. Eschenroeder, A. Q., Boyer, D. W., and Hall, J. G., Nonequilibrium Expansions of Air with Coupled Chemical Reactions. To be published in Phys. Fluids, Vol. 5, No. 5, May 1962.
11. Marrone, P. V. and Eschenroeder, A. Q., Inviscid, Nonequilibrium Flow Behind Bow Shock Waves. Paper presented at the Divisional Meeting of the APS Division of Fluid Dynamics, Berkeley, Calif., November 1961.

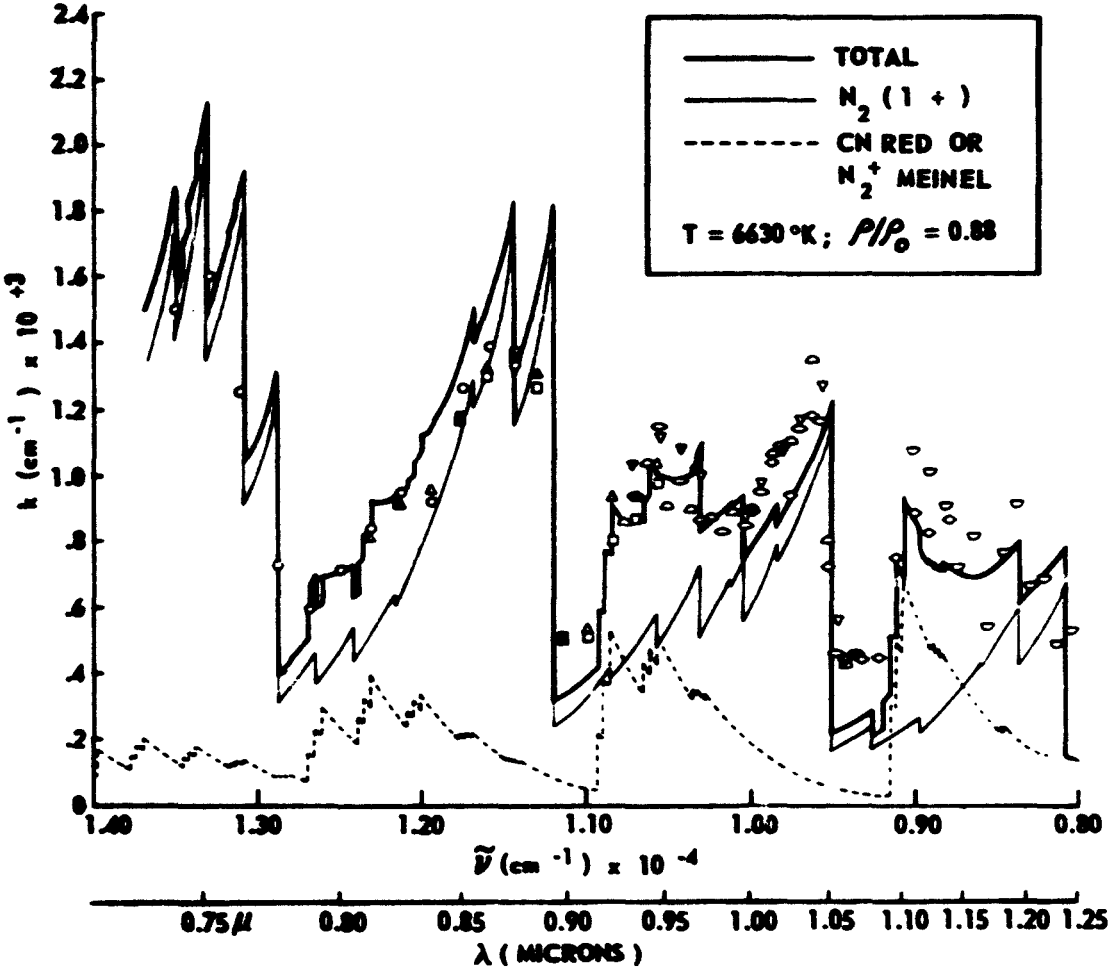

Figure 1 SPECTRAL ABSORPTION COEFFICIENT OF SHOCK-HEATED NITROGEN

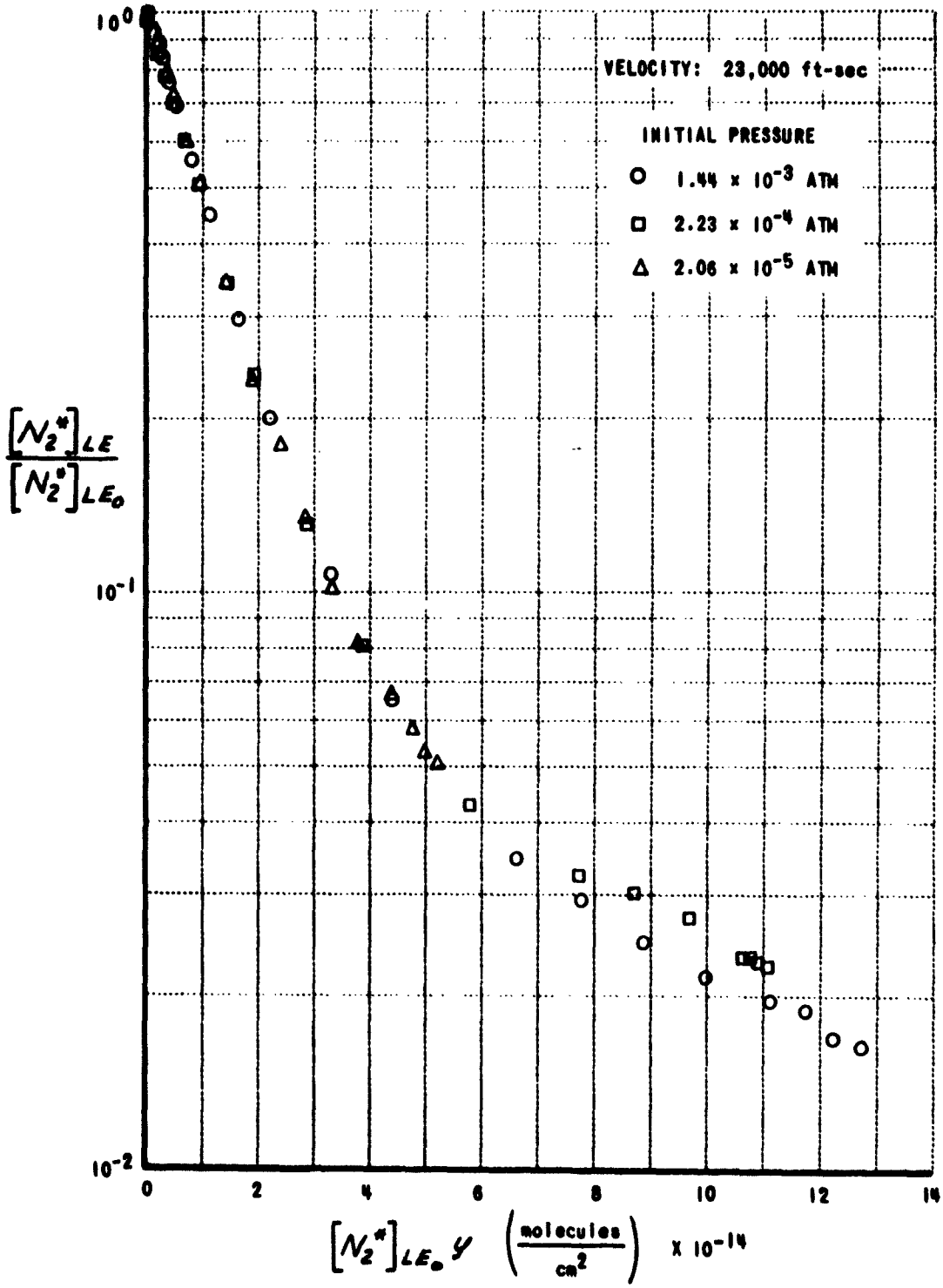

Figure 2 NUMBER DENSITY OF N_2 MOLECULES IN $B^3\Pi$ STATE IN LOCAL EQUILIBRIUM BEHIND NORMAL SHOCKS IN AIR

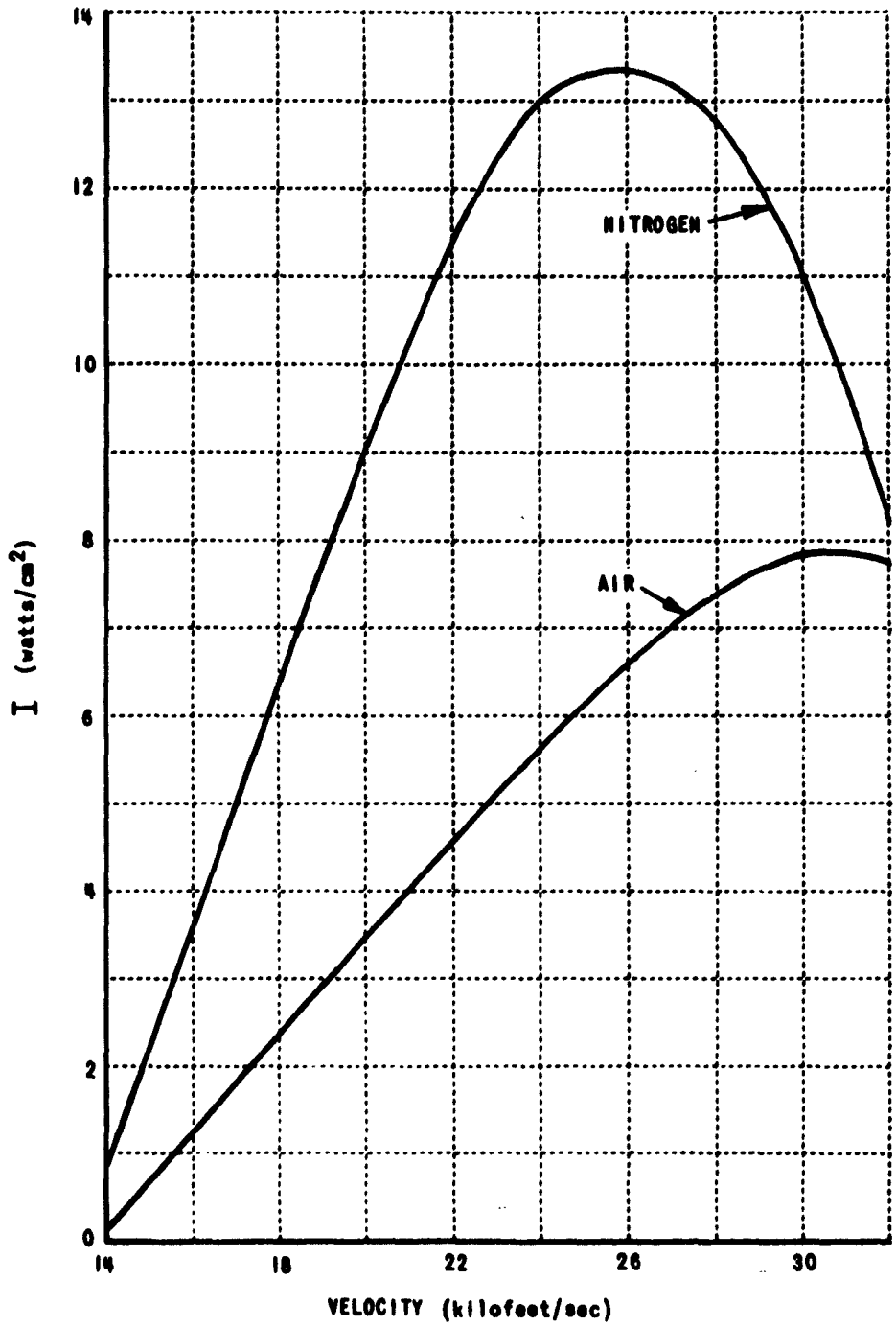

Figure 3 NON-EQUILIBRIUM RADIATION FROM THE $N_2(1+)$ SYSTEM INCLUDING VIBRATIONAL RELAXATION

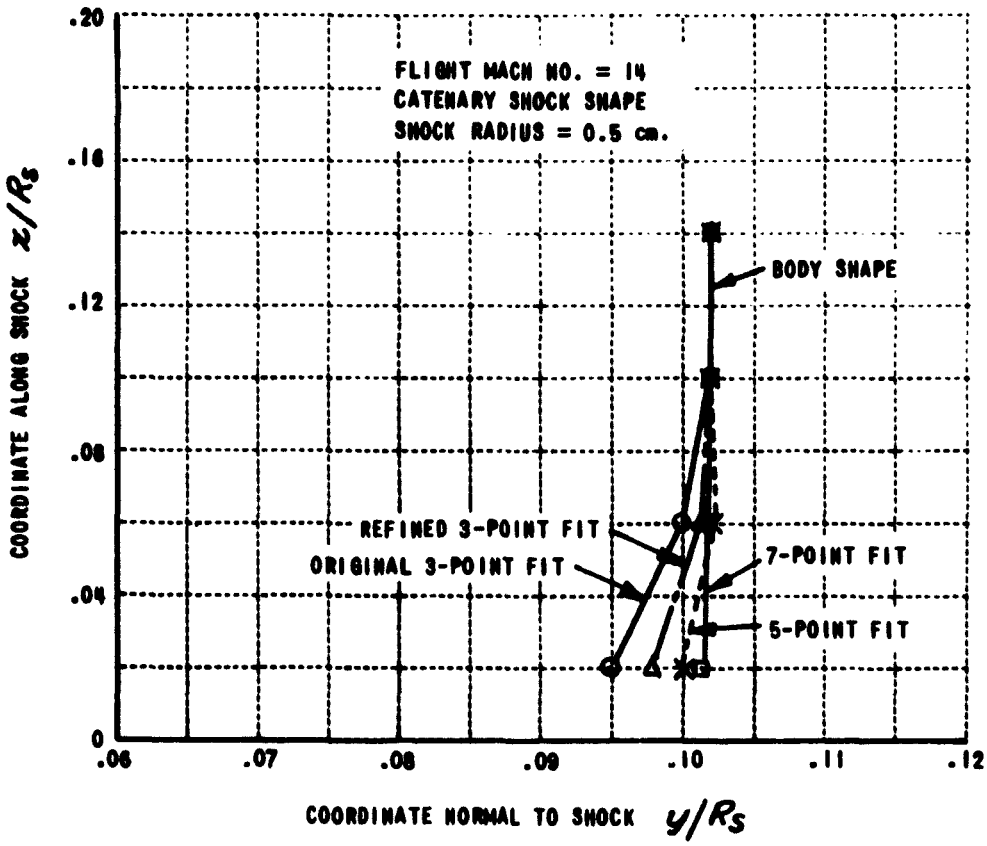

Figure 4 BODY SHAPE NEAR STAGNATION REGION
IDEAL GAS CASE

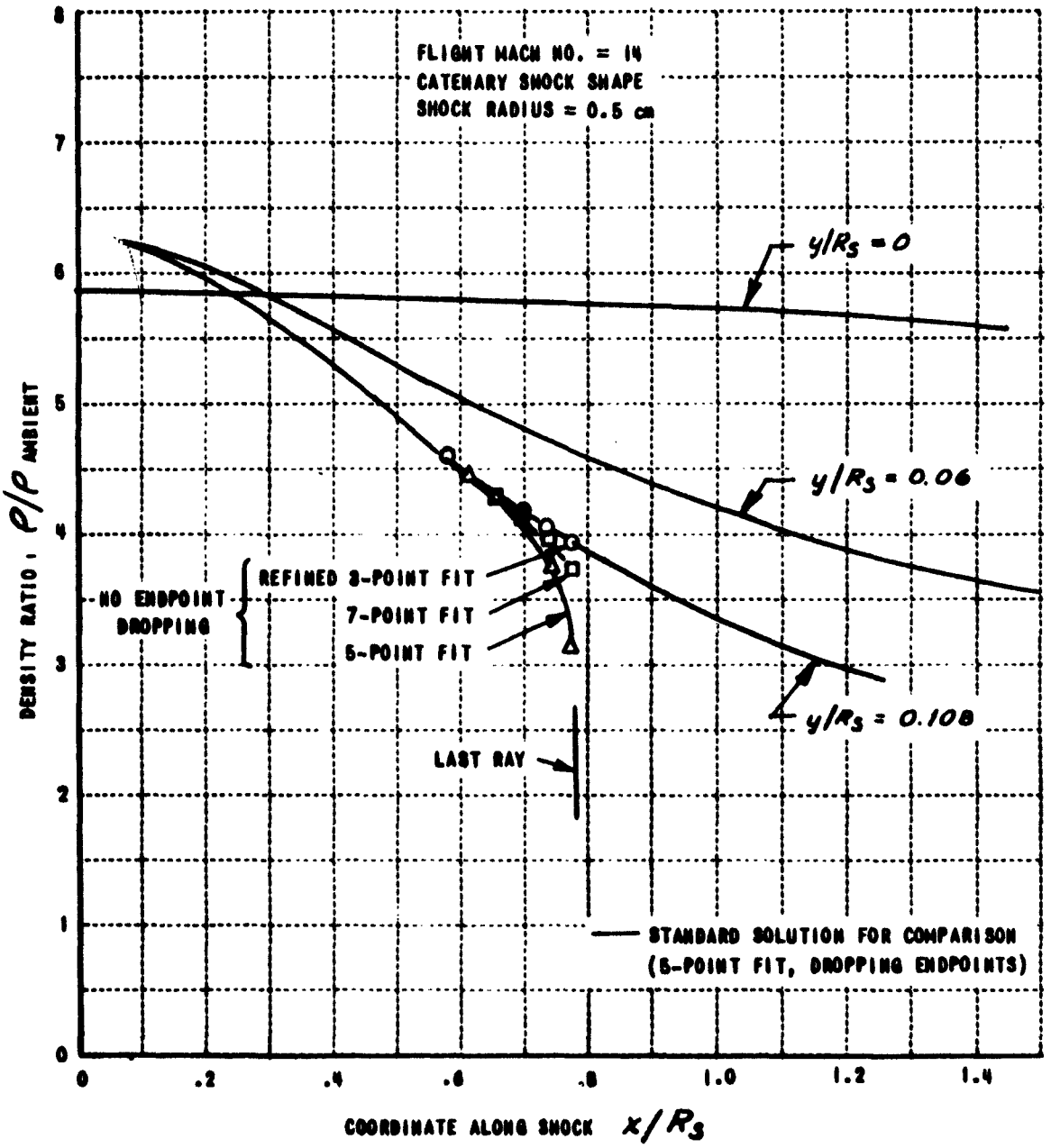

Figure 5 DENSITY DISTRIBUTION BEHIND BOW SHOCK
IDEAL GAS CASE

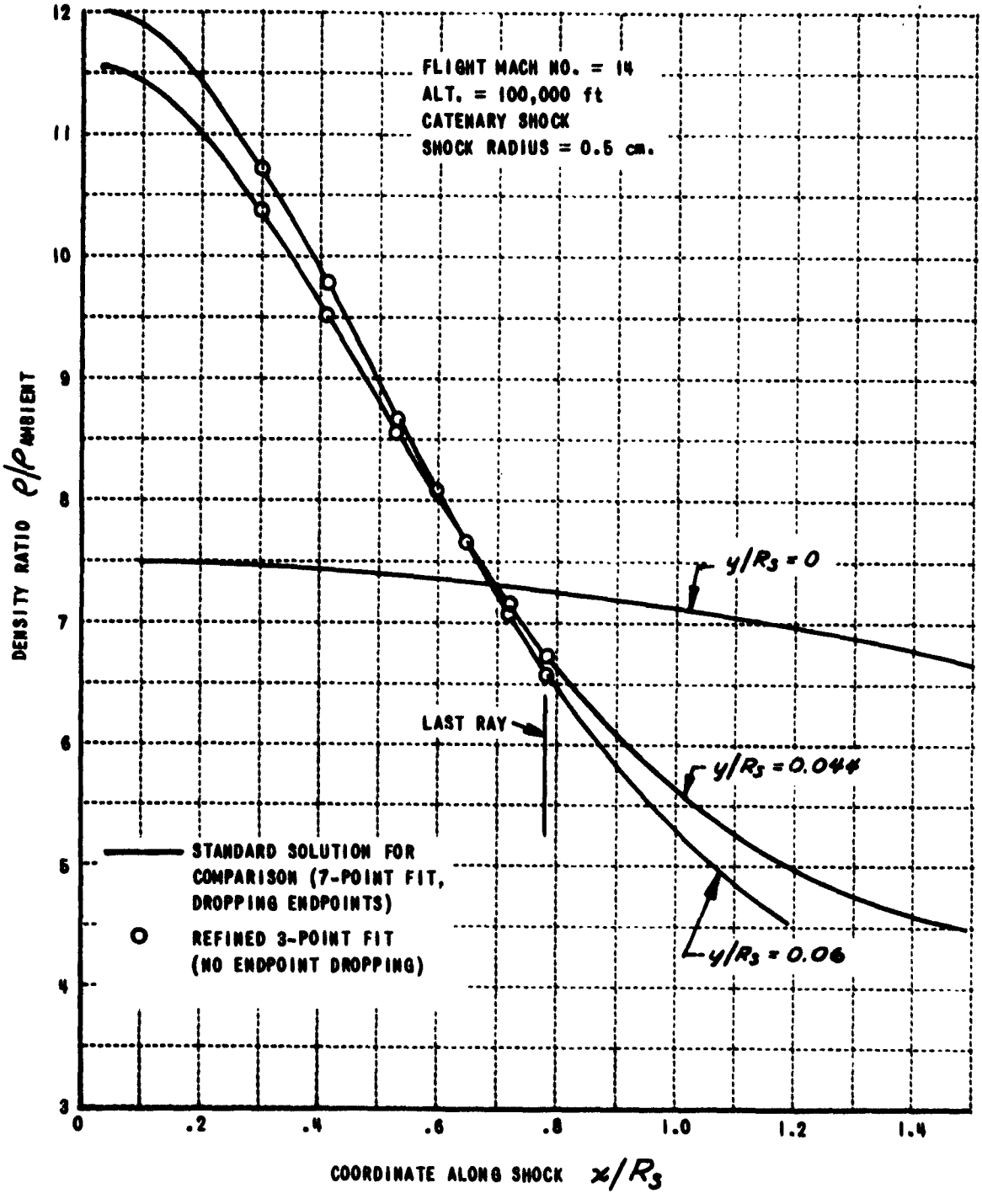

Figure 6 DENSITY DISTRIBUTION BEHIND BOW SHOCK DISSOCIATING OXYGEN CASE

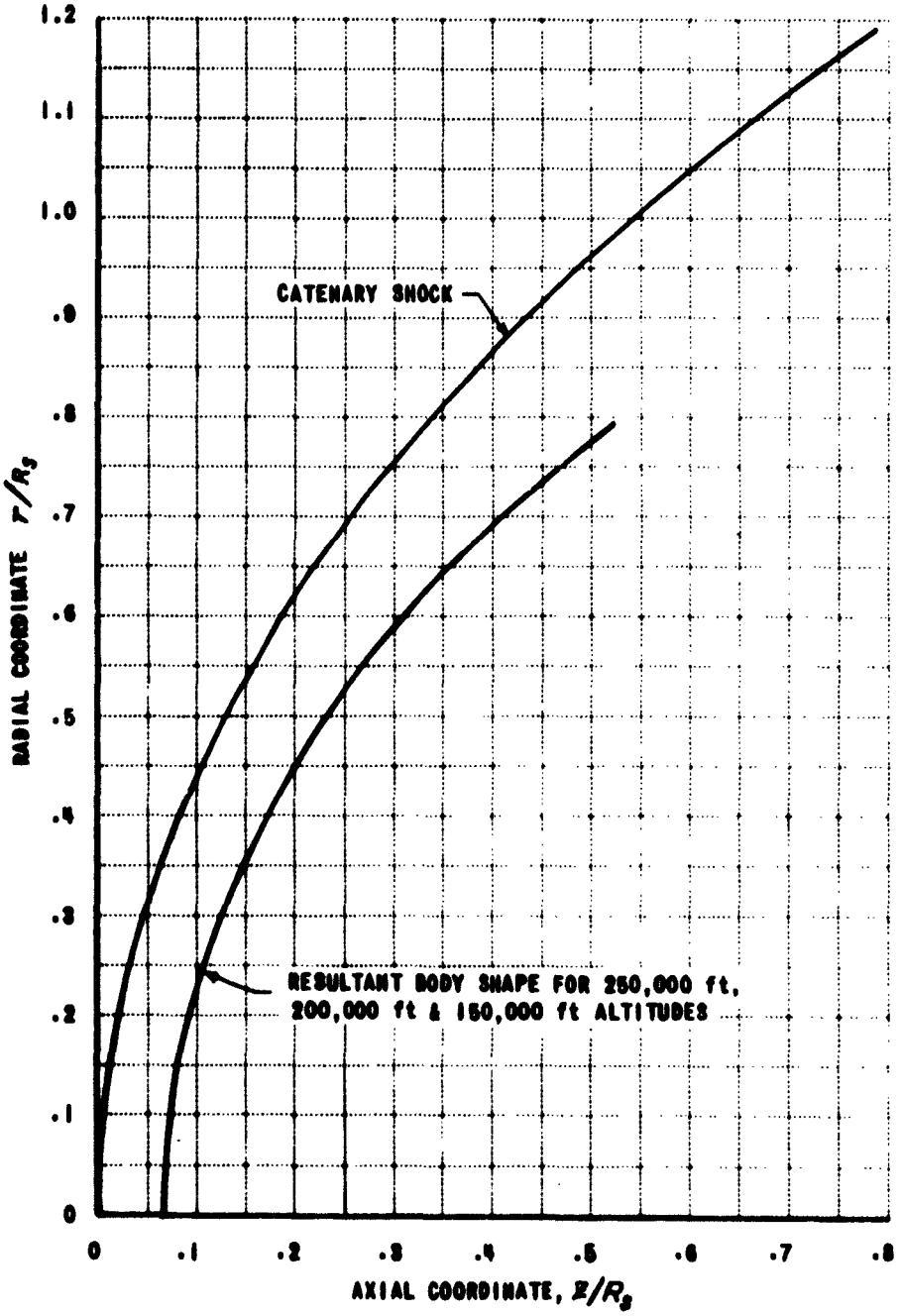

Figure 7 SHOCK LAYER, VELOCITY = 15,000 ft/sec

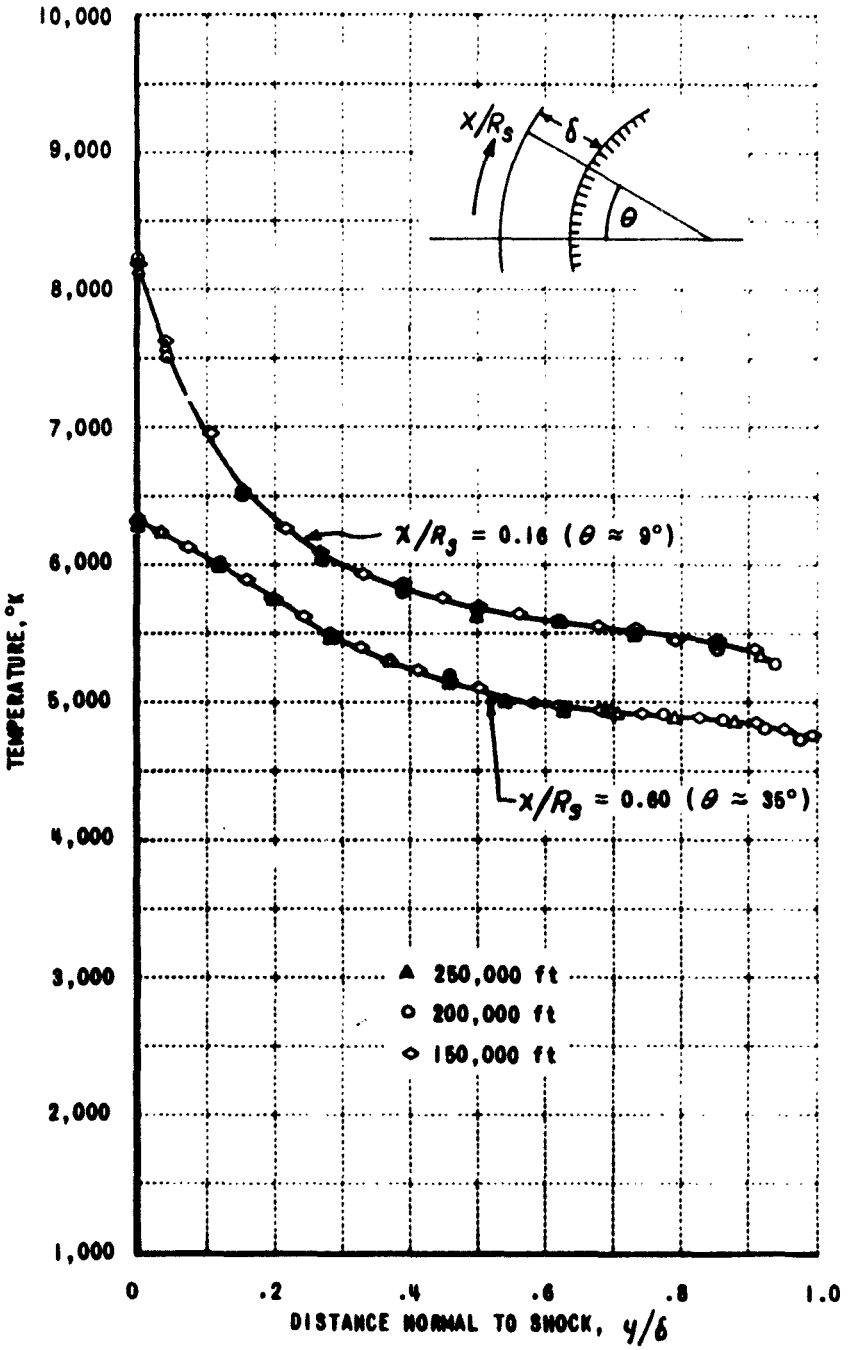

Figure 8 TEMPERATURE DISTRIBUTION BEHIND BOW SHOCK
VELOCITY = 15,000 ft/sec

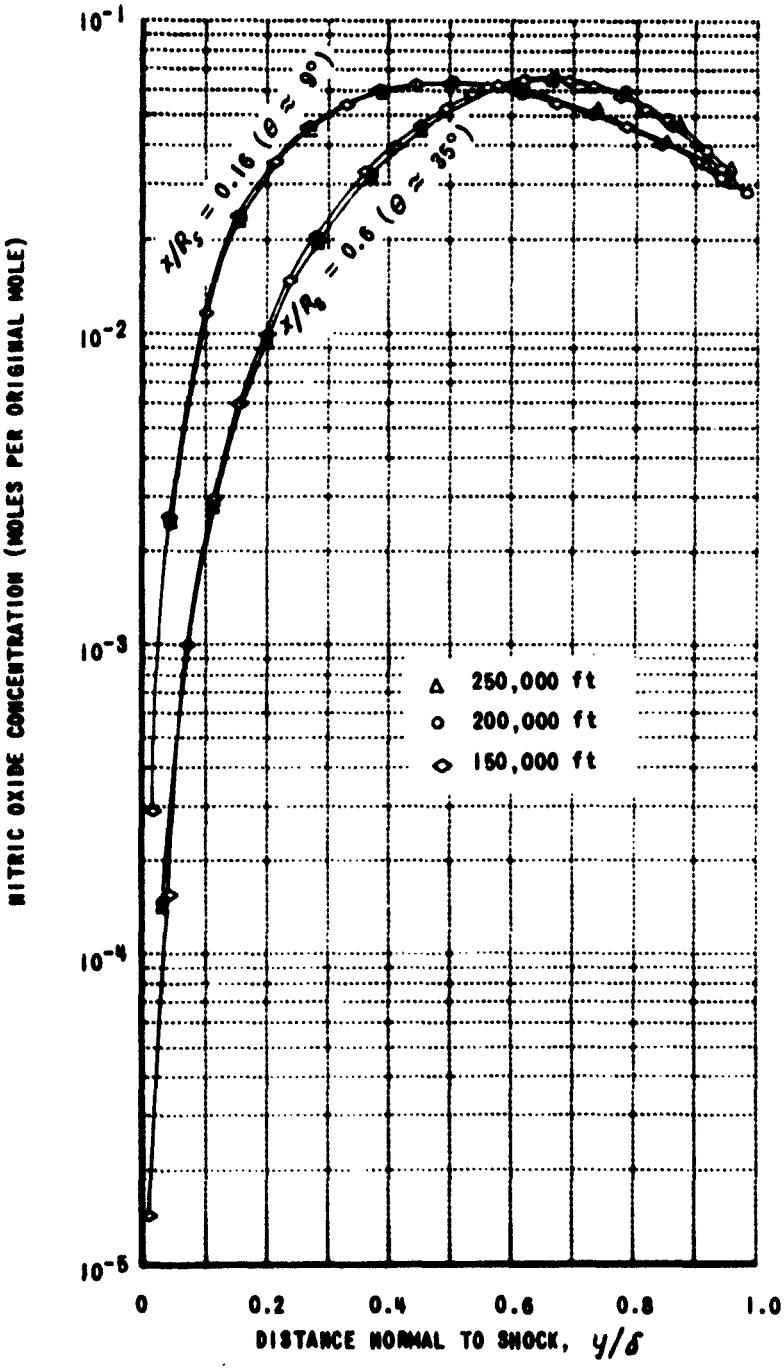

Figure 9 NITRIC OXIDE (NO) CONCENTRATION BEHIND BOW SHOCK WAVE VELOCITY = 15,000 ft/sec

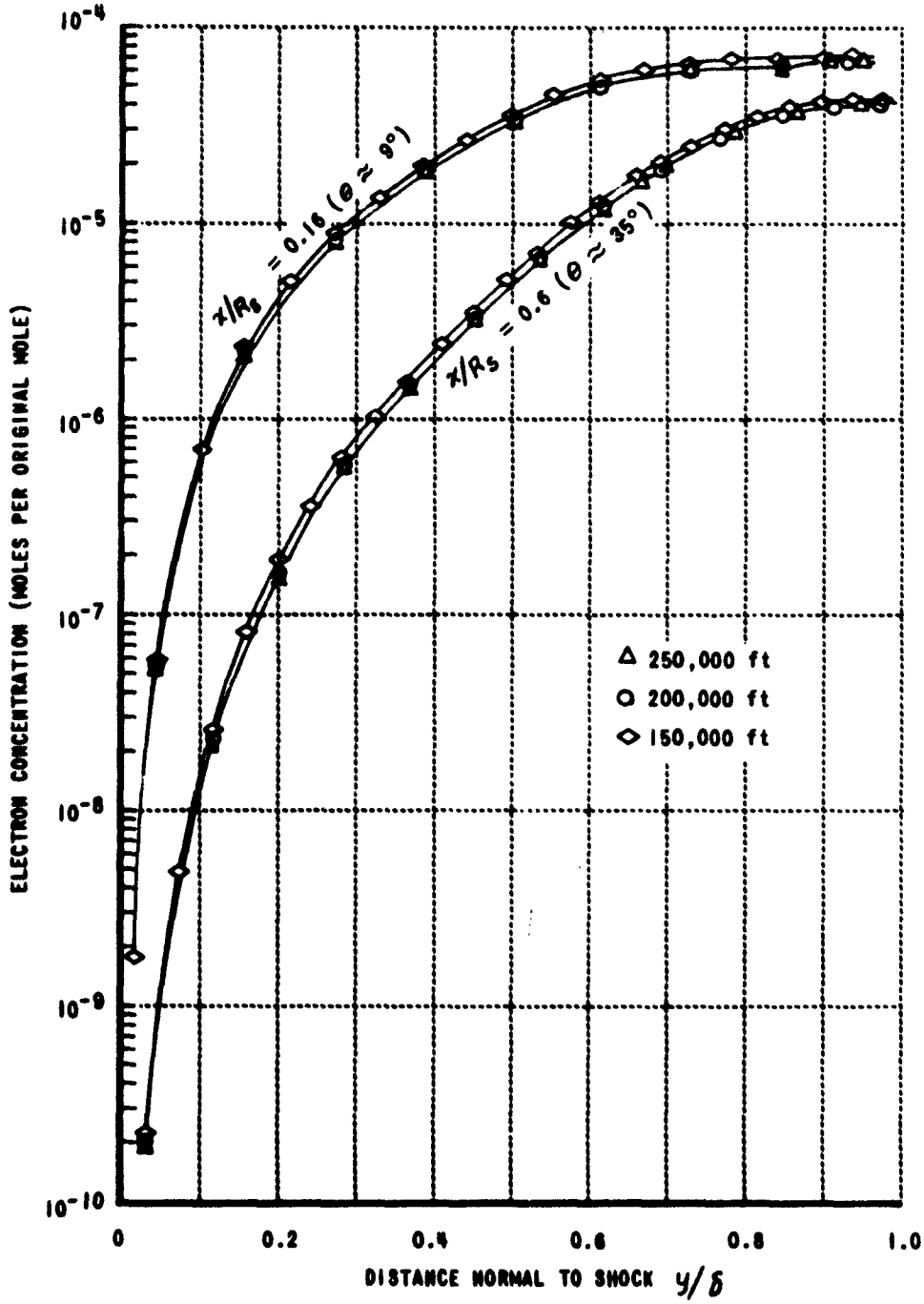

Figure 10 ELECTRON (e^-) CONCENTRATION BEHIND BOW SHOCK WAVE
VELOCITY = 15,000 ft/sec

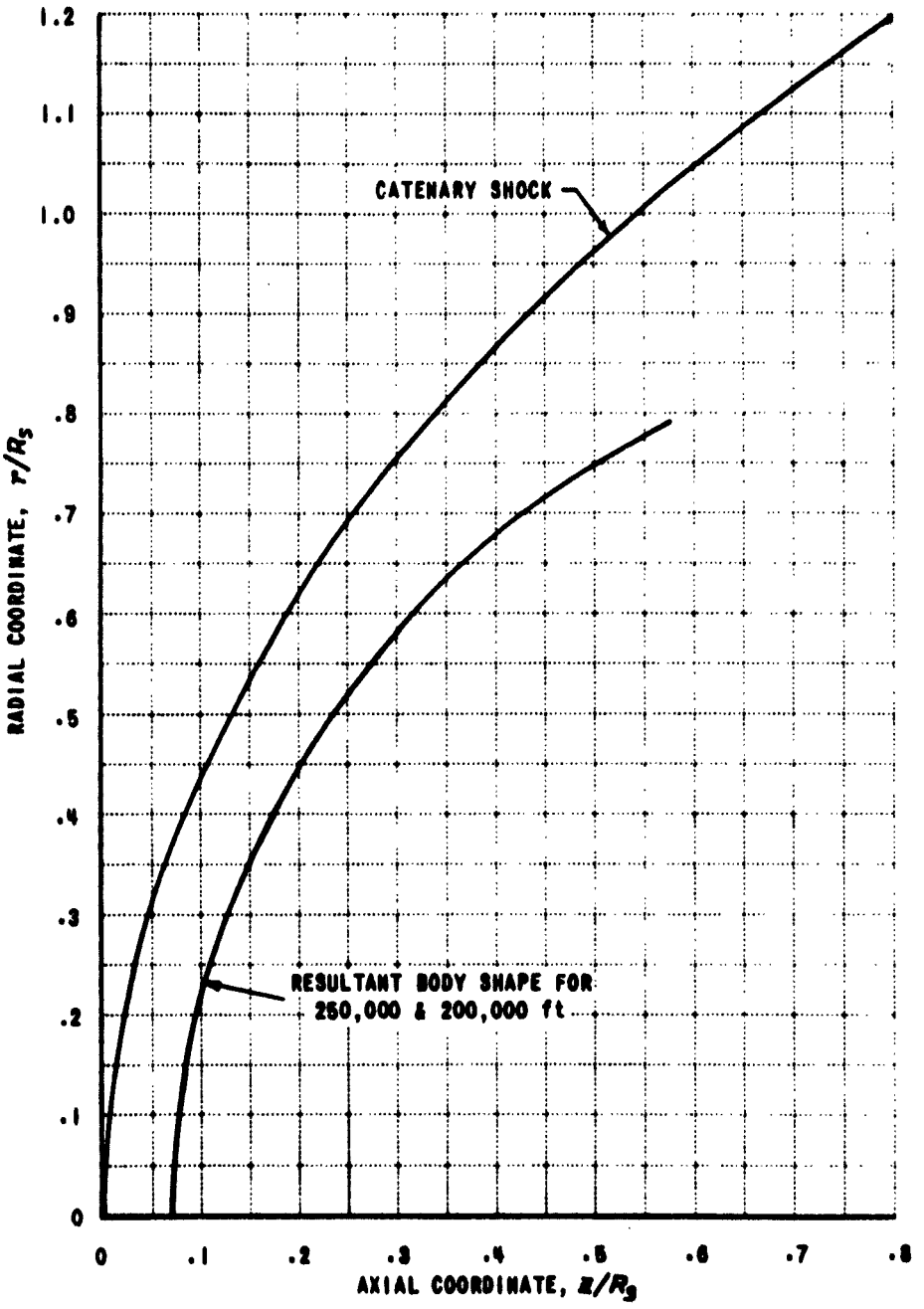

Figure 11 SHOCK LAYER, VELOCITY = 23,000 ft/sec

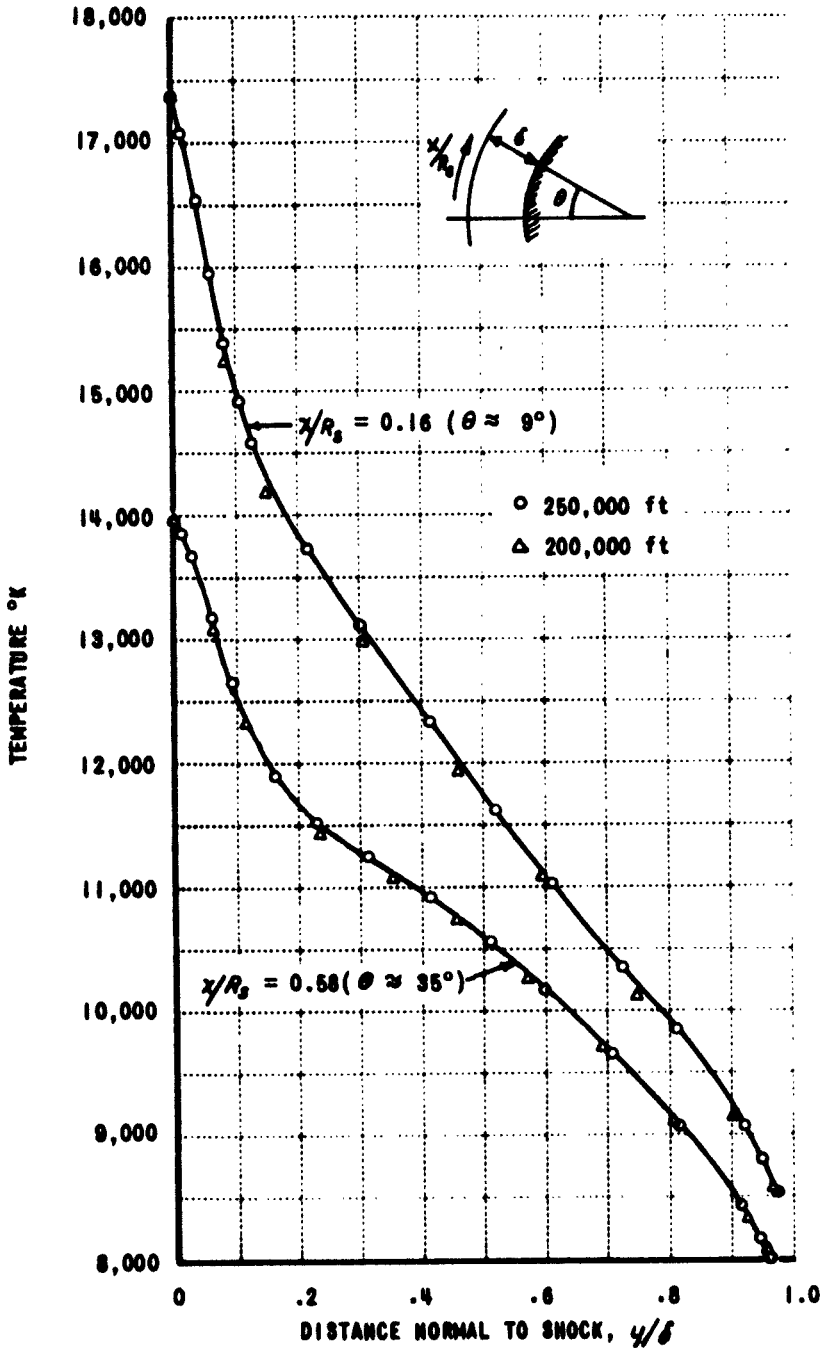

Figure 12 TEMPERATURE DISTRIBUTION BEHIND BOW SHOCK
VELOCITY = 23,000 ft/sec

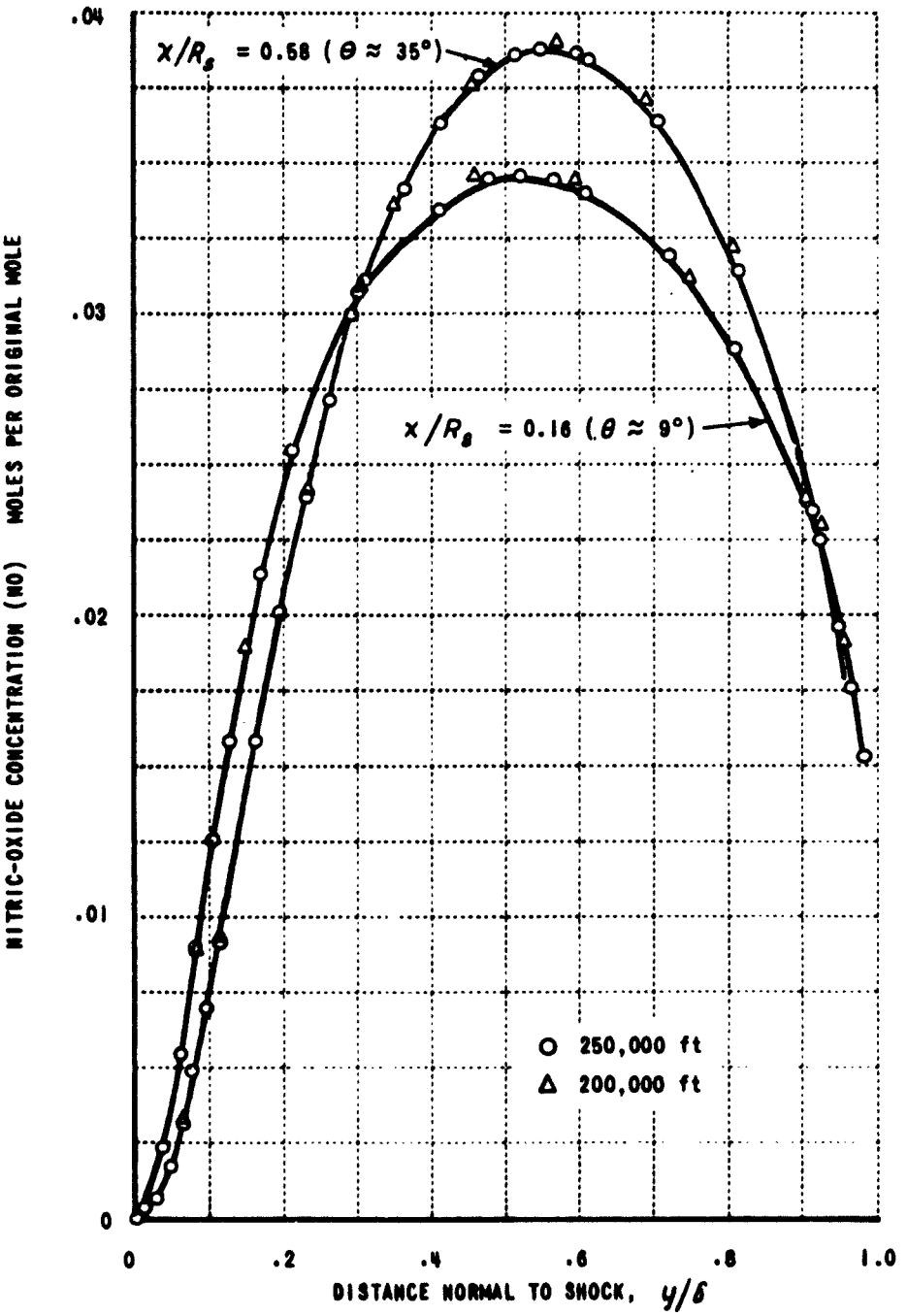

Figure 13 NITRIC-OXIDE DISTRIBUTION BEHIND BOW SHOCK
VELOCITY = 23,000 ft/sec

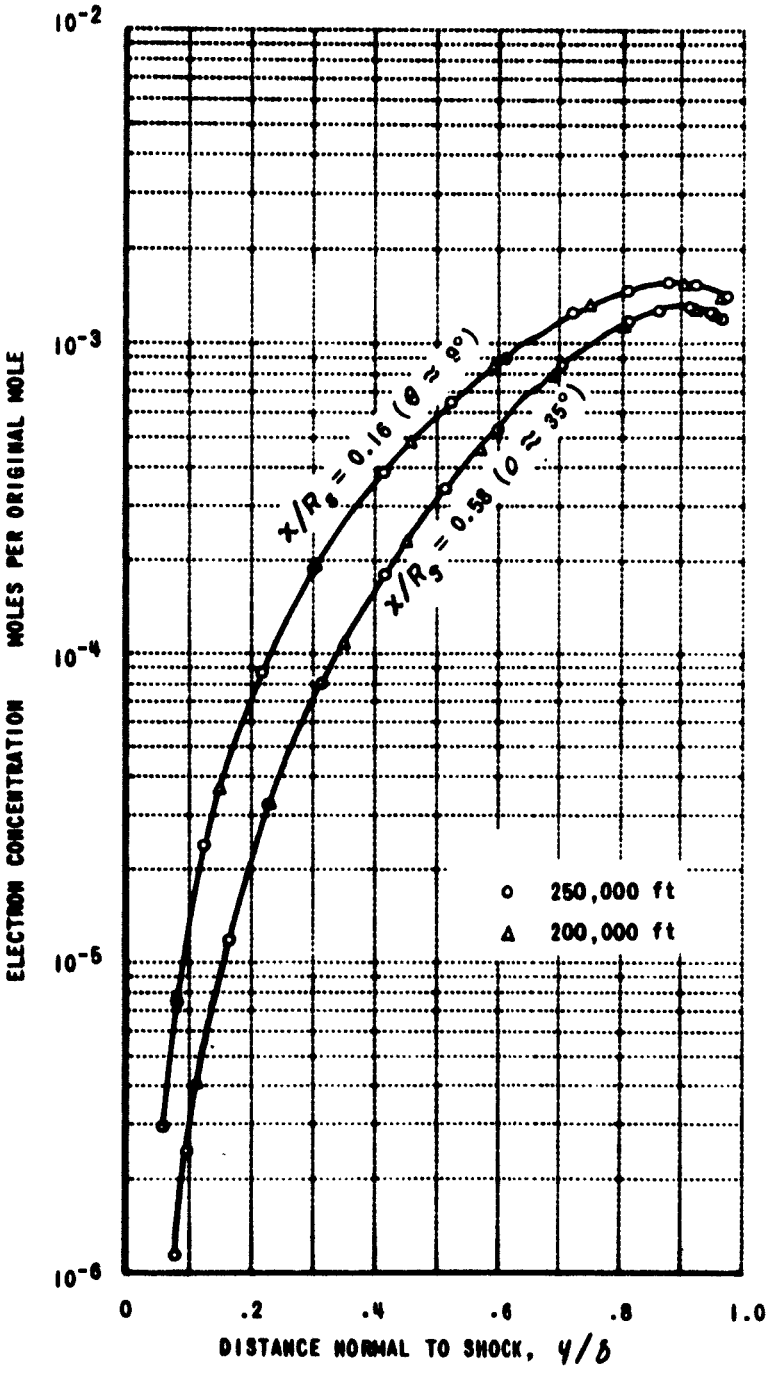

Figure 14 ELECTRON CONCENTRATION BEHIND BOW SHOCK
VELOCITY = 23,000 ft/sec

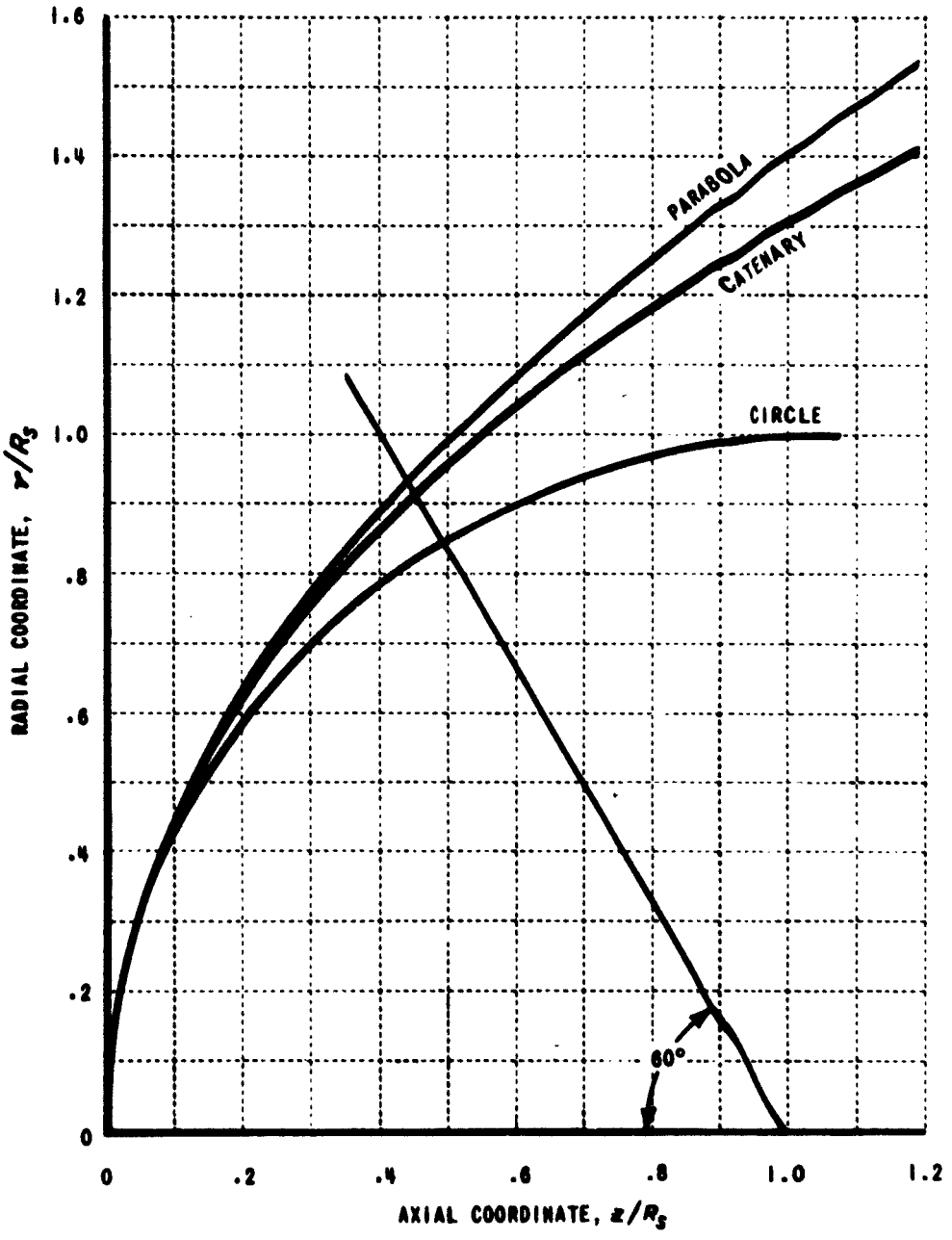

Figure 15 BOW SHOCK SHAPES

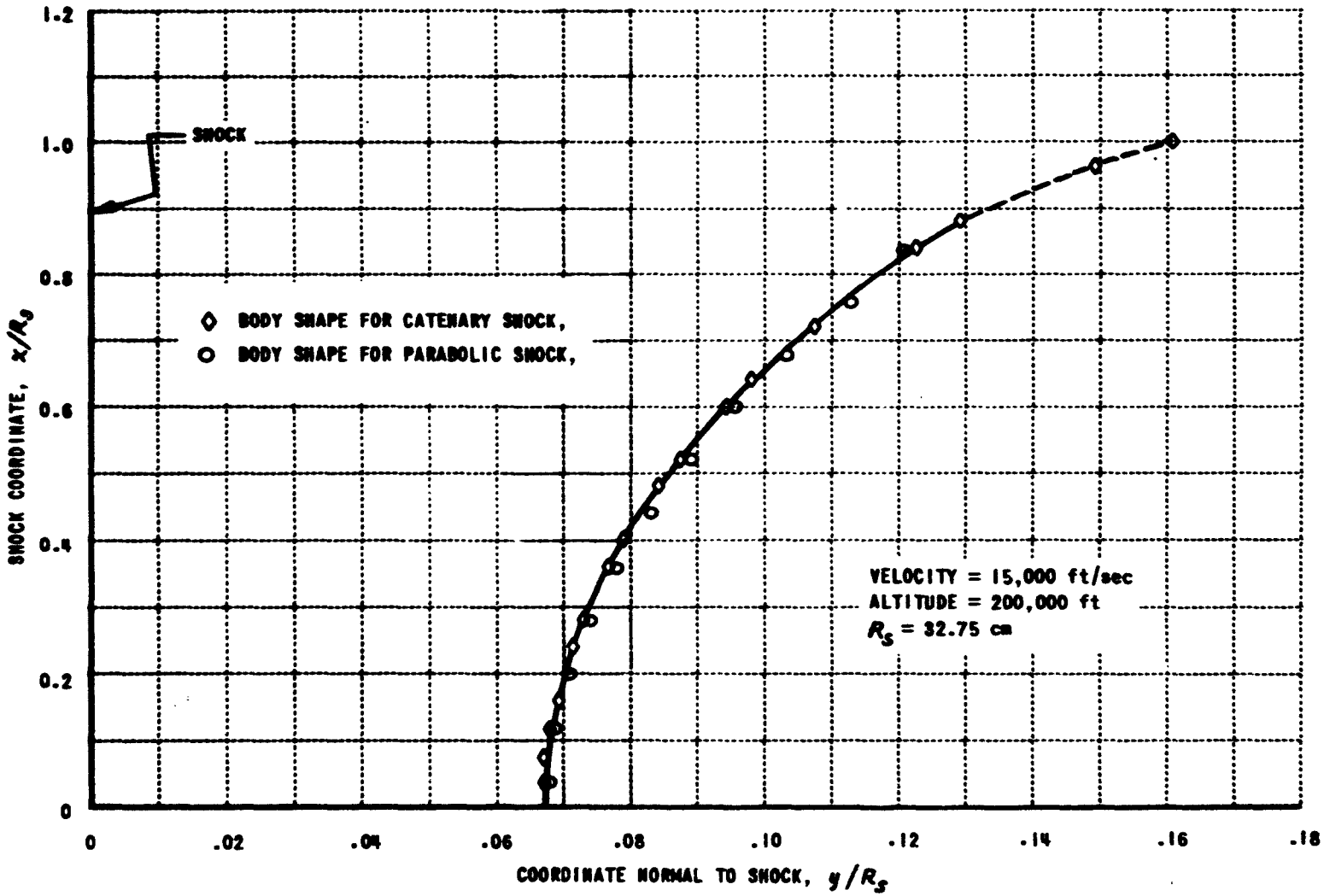

Figure 16 BODY SHAPE IN SHOCK COORDINATE SYSTEM

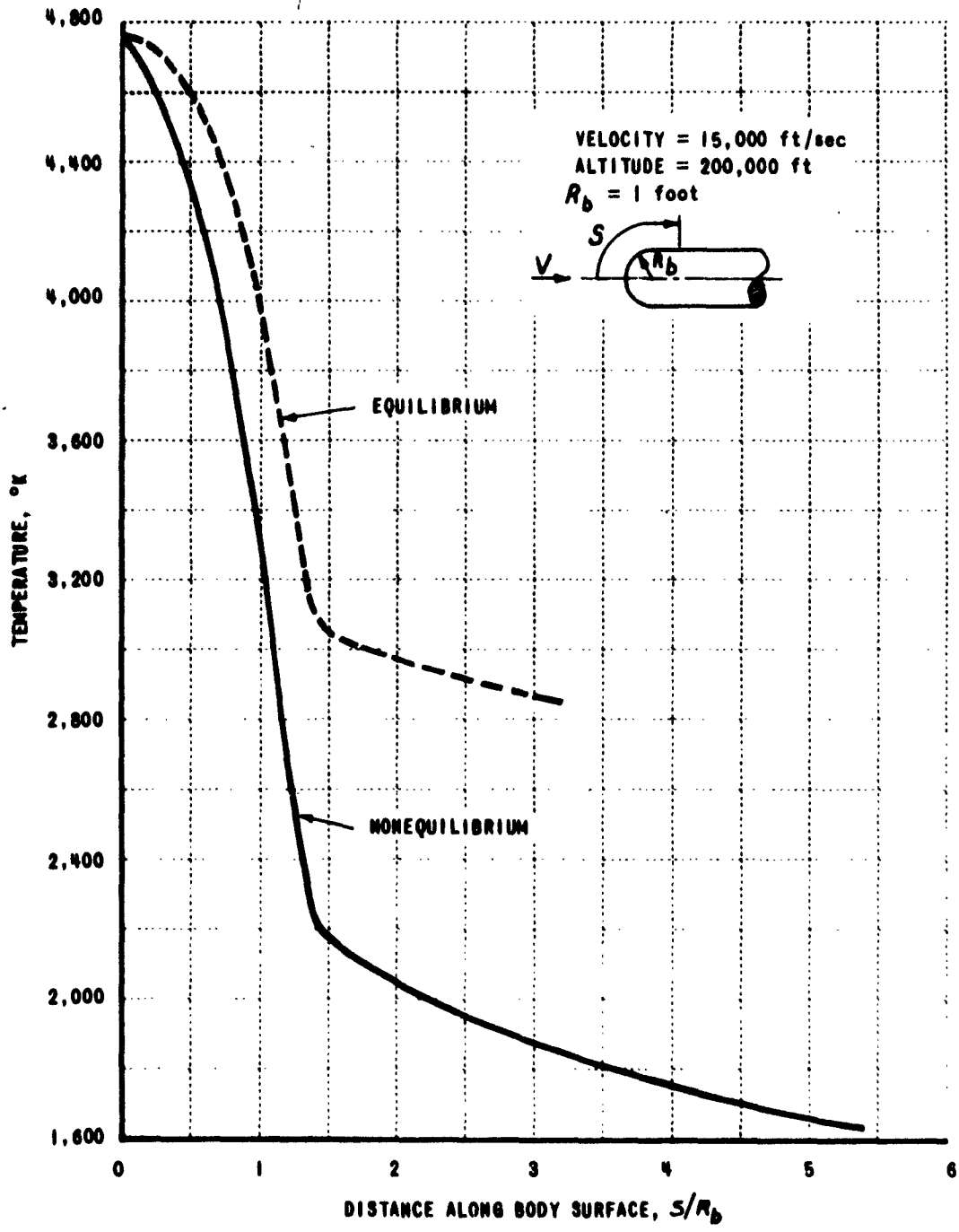

Figure 17 TEMPERATURE VARIATION ALONG SURFACE STREAMLINE OF HEMISPHERE CYLINDER

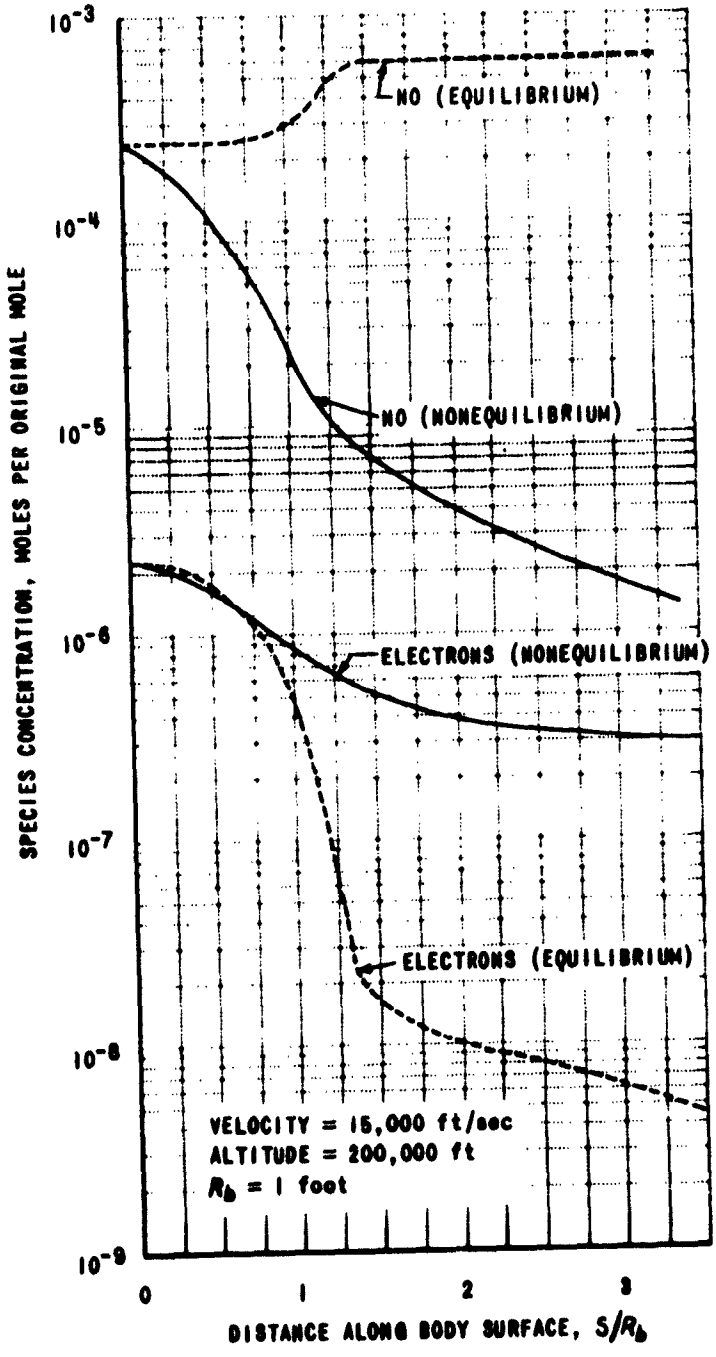

Figure 18 NITRIC-OXIDE(NO) AND ELECTRON CONCENTRATION ALONG SURFACE STREAMLINE OF HEMISPHERE CYLINDER

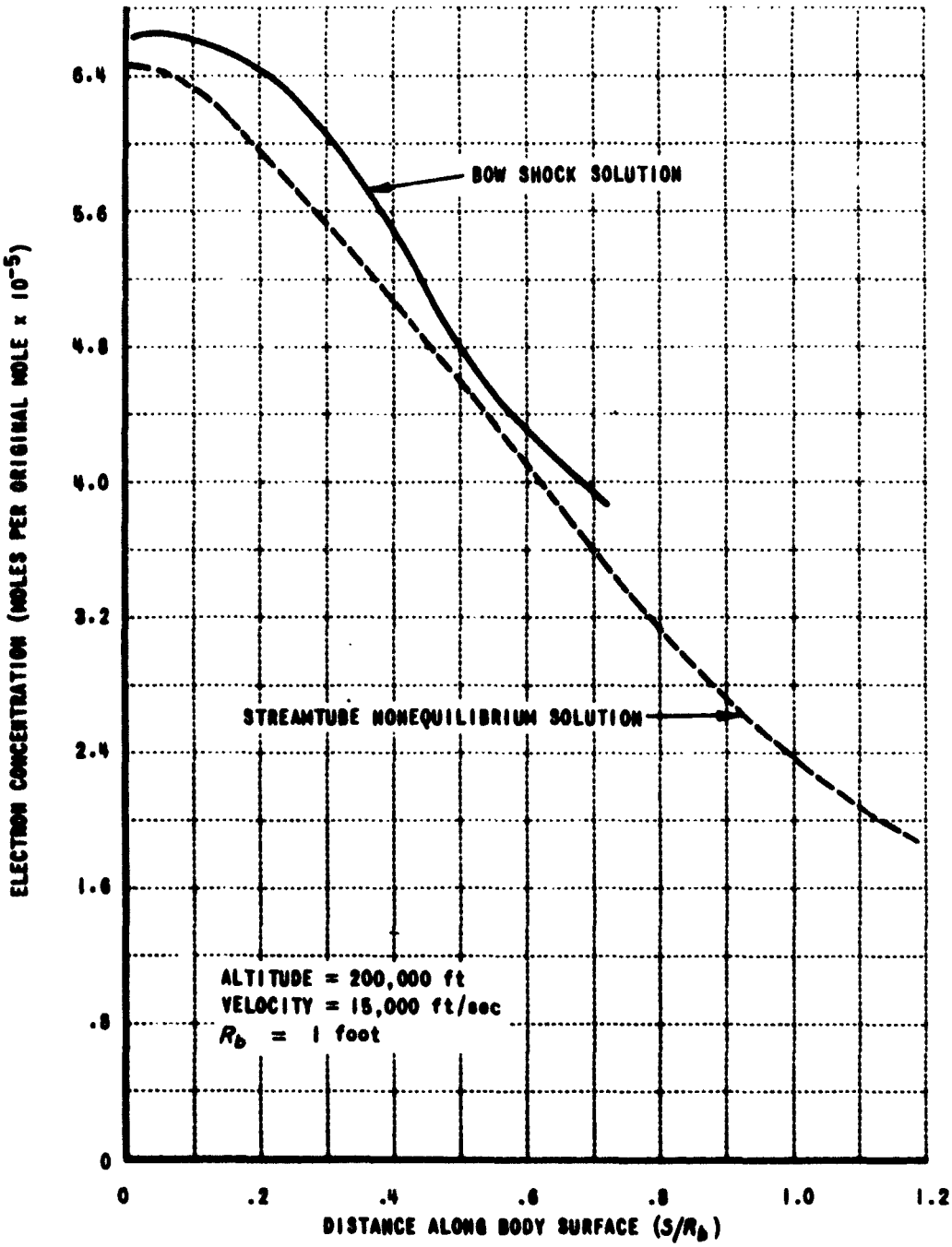

Figure 19 COMPARISON OF STREAMTUBE APPROXIMATION WITH BOW SHOCK SOLUTION ELECTRON CONCENTRATION ALONG SURFACE OF BODY

APPENDIX A

Measured Transition Probability for the First-Positive Band System of Nitrogen*

Walter H. Wurster
Cornell Aeronautical Laboratory, Inc., Buffalo, New York

ABSTRACT

The electronic transition probability for the nitrogen first-positive system has been obtained from absolute spectral-intensity measurements of the infrared radiation from shock-heated nitrogen. A twelve-channel spectrometer was used, whose resolution was sufficient to separate the vibrational band sequences. The temperature dependence of the spectrum was shown to agree with that determined for nitrogen in thermodynamic equilibrium. An electronic transition moment $|R_e|^2$ equal to 0.096 atomic units and independent of internuclear separation gave the best fit to the data. The measured intensities are shown to be lower by a factor of five than those reported for measurements in shock-heated air, and the corresponding f-number, evaluated at 9512 $cm^{-1}(v'=0, v''=0)$, was found to be $(2.8 \pm 0.7) \times 10^{-3}$. A second component of radiation was detected, and shown to be attributable to either the CN red or N_2^+ Meinel band systems.

---

* This research is a part of Project Defender, sponsored by the Advanced Research Projects Agency, Department of Defense.

APPENDIX B

Inviscid Hypersonic Airflows With Coupled Nonequilibrium Processes*

J. Gordon Hall,[1] Alan Q. Eschenroeder,[2] and Paul V. Marrone[3]

Cornell Aeronautical Laboratory, Inc., Buffalo, New York

ABSTRACT

Analyses have been made of the effects of coupled chemical rate processes in external and internal inviscid hypersonic airflows at high enthalpy levels. Exact (numerical) solutions have been obtained by the inverse method for inviscid airflow over a blunt nose under flight conditions where nonequilibrium prevails through the nose region. Numerical solutions have also been obtained for nonequilibrium expansions of air from initial equilibrium states appropriate to afterbody flows in flight and to hypersonic nozzle airflows. The results illustrate the general importance of the coupling among the reactions considered. These included dissociation-recombination,

---

* This work was supported by the Office of Scientific Research, Mechanics Division, under Contract No. AF 49(638)-792; is a part of Project Defender, sponsored by the Advanced Research Projects Agency, Department of Defense; and by CAL Internal Research.

1. Assistant Head, Aerodynamic Research Department.

2. Research Aeronautical Engineer.

3. Research Aerodynamicist.

bimolecular exchange, and ionization reactions. In blunt-nose flow the NO exchange reactions are important for the kinetics of NO and N. In the regime studied, where nonequilibrium prevails through the nose region, atom concentrations tend to freeze at levels below infinite-rate equilibrium. The kinetics are dominated by two-body collision processes. As a consequence, the entire inviscid airflow including coupled nonequilibrium phenomena can be scaled at given velocity on the basis of a constant product of ambient density and body scale. This similitude, which can also be employed for scaling of viscous and radiation phenomena in the shock layer, provides a useful flexibility for hypersonic testing where applicable.

In air expansions from equilibrium, the NO exchange reactions can provide significant equilibration of nitrogen dissociation. Particularly in hypersonic nozzle airflows, the exchange path for N-atom removal can recover a large fraction of the total enthalpy which would otherwise be frozen with three-body recombination alone. Good agreement is obtained between present calculations and experimental static-pressure measurements of Nagamatsu et al for air expansions where O-atom freezing dominates. With respect to hypersonic testing, the present studies indicate nozzle freezing to be a serious problem for simulation of flight nonequilibrium phenomena appropriate to small scale and high altitudes. Nozzle-flow nonequilibrium is minimized by high pressures. Where applicable, the binary scaling above may be useful in this respect.